

# SPACE-WEIGHTED SEISMIC ATTENUATION MULTI-FREQUENCY TOMOGRAPHY AT DECEPTION ISLAND VOLCANO (ANTARTICA)

Roberto Guardo\*, L. De Siena, A. Caselli, J. Prudencio, G. Ventura.



# Index

- Theory and Method

- Analysis

- Results

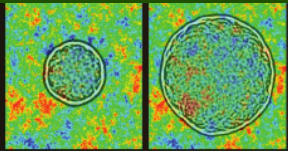
- Discussions

- Outlooks



# THEORY 1/2

The “Japanese School”  
energy variations in the  
heterogeneous Earth



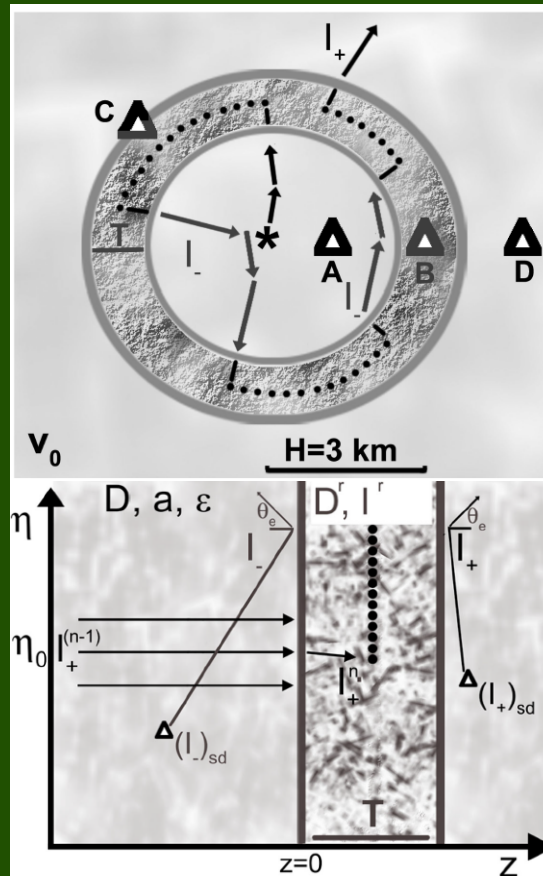
Haruo Sato · Michael C. Fehler  
Takuto Maeda

Seismic Wave  
Propagation and  
Scattering in  
the Heterogeneous  
Earth

Second Edition

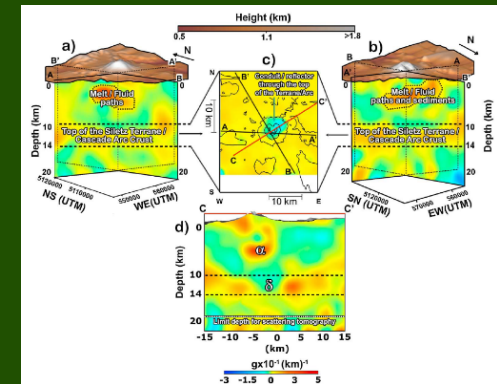
Springer

The “framework”:  
building forward  
models with Radiative  
Transfer Theory

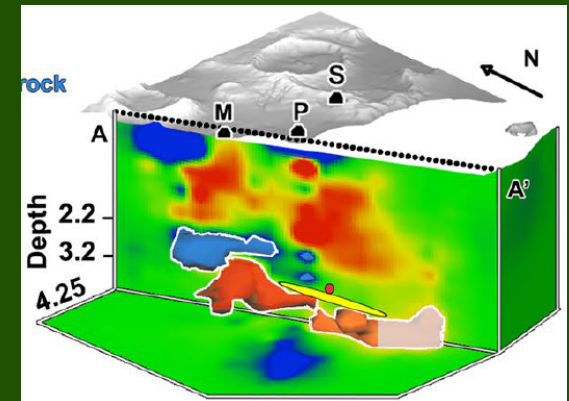


Seismic attenuation  
tomography in  
volcanoes

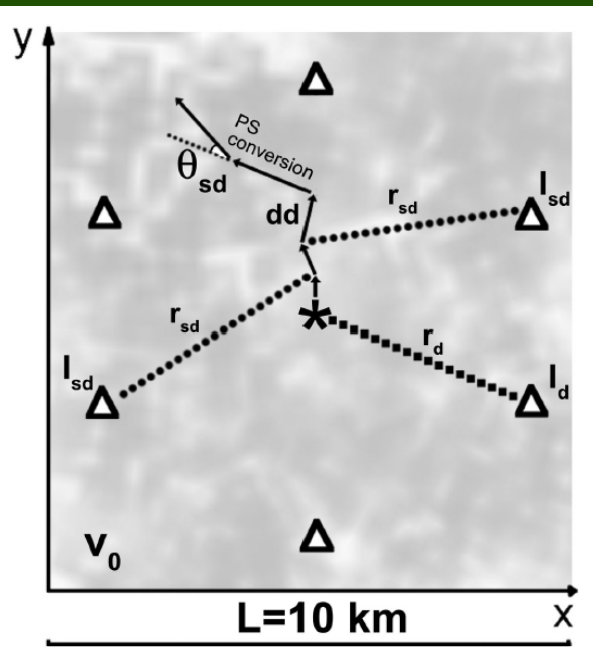
Mount St. Helens



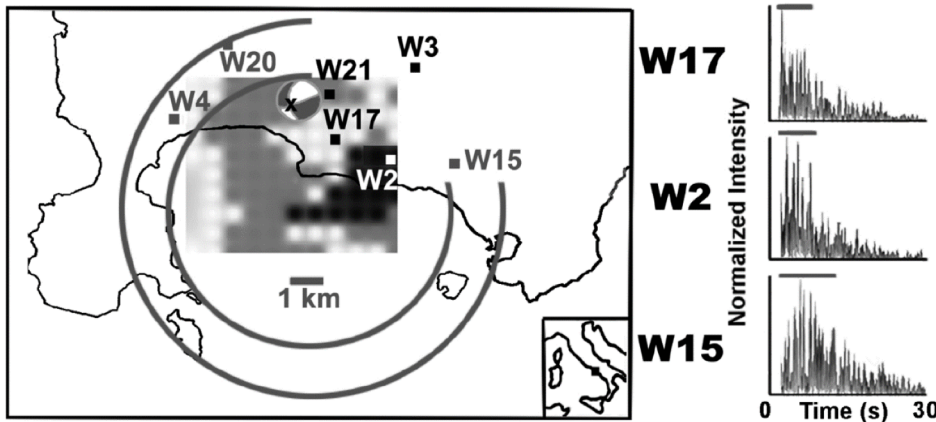
Campi Flegrei



# THEORY 2/2



- Applying the **theory of radiative transfer**, sensitivity kernels can be obtained by modeling scattering intensities at different lapse times;
- Use coda-wave "scattered" information;
- Absorption + scattering → **Coda Quality Factor ( $Q_c$ )**;
- $Q_c$  is measured from the decay of coda intensity versus lapse time.

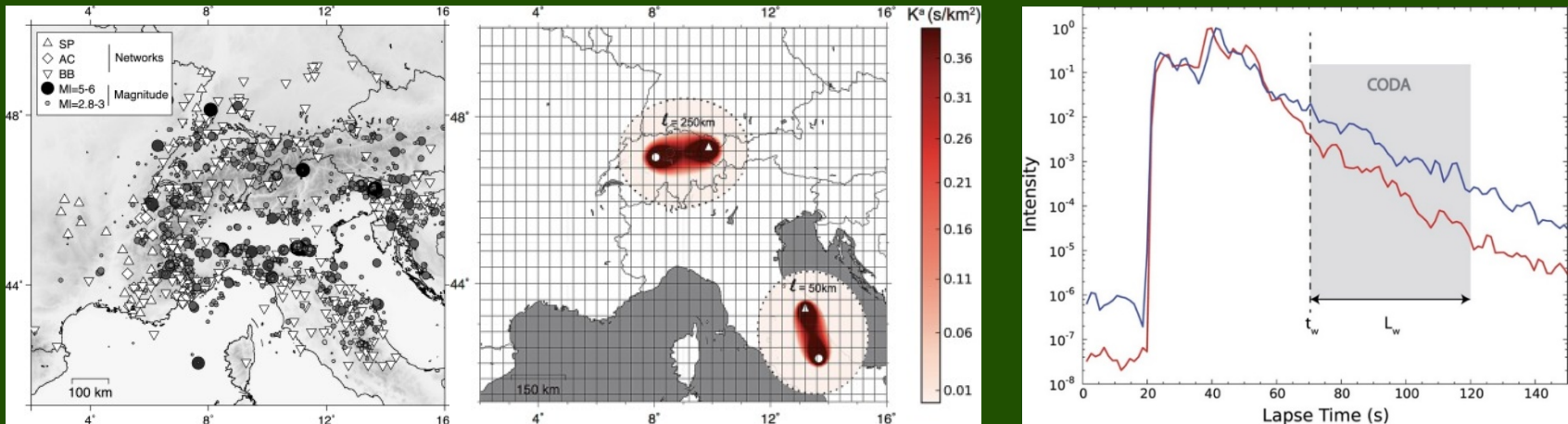


- Does not work at all frequencies and scales at the same way:  
**we need results in different frequency bands.**

# METHOD 1/3

## SENSITIVITY KERNELS FOR CODA IMAGING: REGIONAL/CONTINENTAL SCALES

(MAYOR ET AL. 2016)



Linear relation between  
the spatial variation of the inelastic quality factor  $Q_i(\mathbf{x})$  and  $Q_c$ :

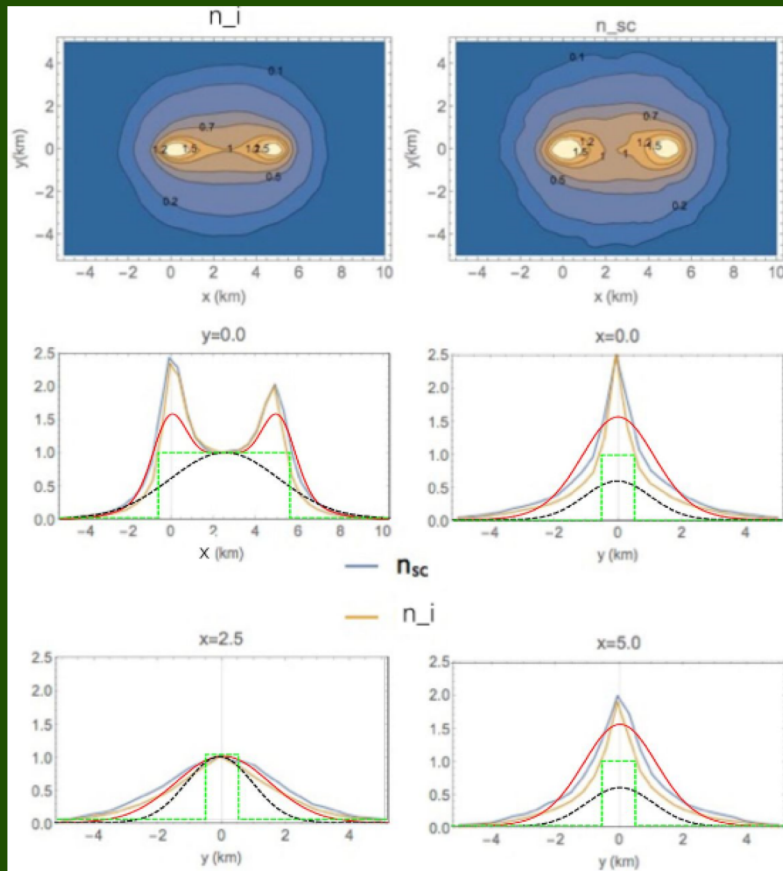
$$Q_c^{-1}(\mathbf{R}, \mathbf{S}) \approx \frac{\int Q_i^{-1}(\mathbf{x}) K_a(\mathbf{R}, \mathbf{S}; \mathbf{x}, t) d\mathbf{x}}{t}$$

“ $K_a$ ”, the absorption sensitivity kernel, which depends on the position of the source ( $\mathbf{S}$ ) and receiver ( $\mathbf{R}$ ) and the lapse-time  $t$  in the coda.

# METHOD 2/3

## KERNELS-BASED IMAGING IN VOLCANOES

(DEL PEZZO ET AL. 2016)



Inhomogeneous scattering properties of volcanoes to map shape and dimensions of hot reservoirs and plumbing systems.

The **forward model** is built with Monte Carlo simulations of Radiative Transfer Theory equations.

Sensitivity is generally **maximum at source and receiver**, with wider illumination than in ray-dependent tomography.



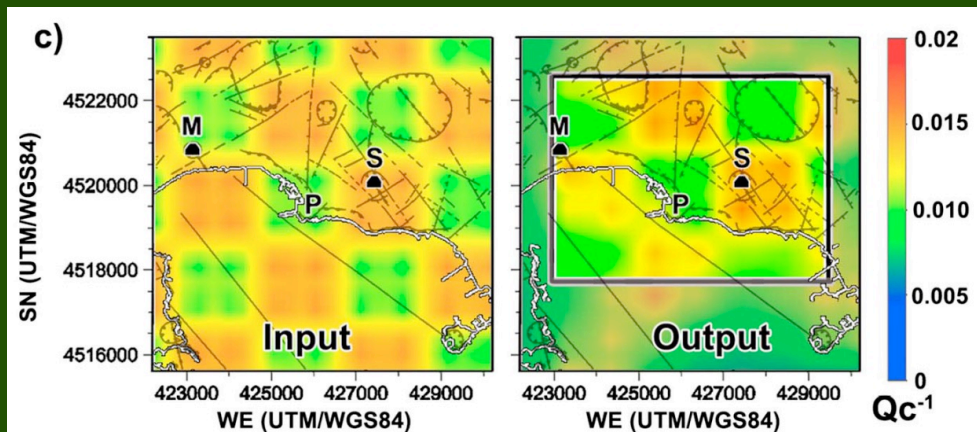
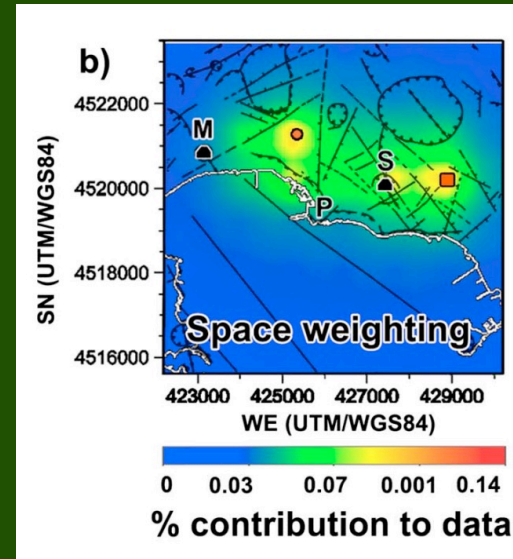
# METHOD 3/3

## KERNELS-BASED IMAGING IN VOLCANOES (INVERSION MODEL)

(DE SIENA ET AL. 2017)

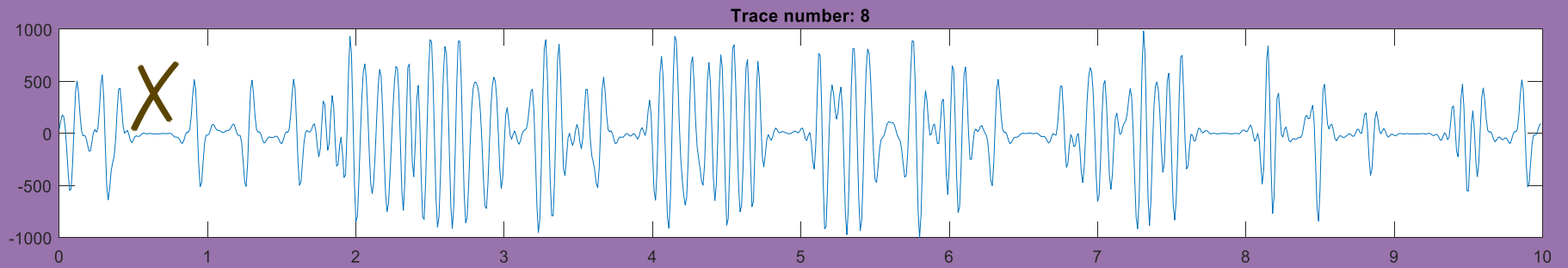
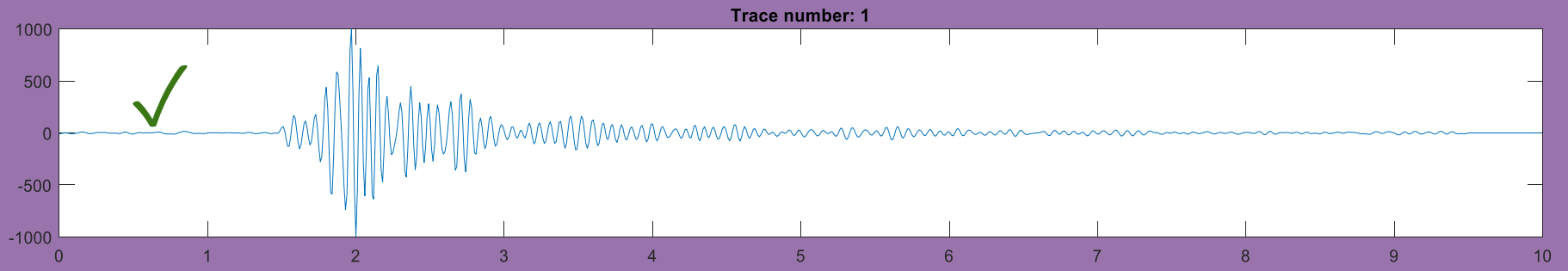
The main assumption is that total coda attenuation is caused by the medium comprising the inversion grid;

The weighting functions provide the rows of the inversion matrix at the nodes after normalization for the total weight relative to the source-receiver pair;

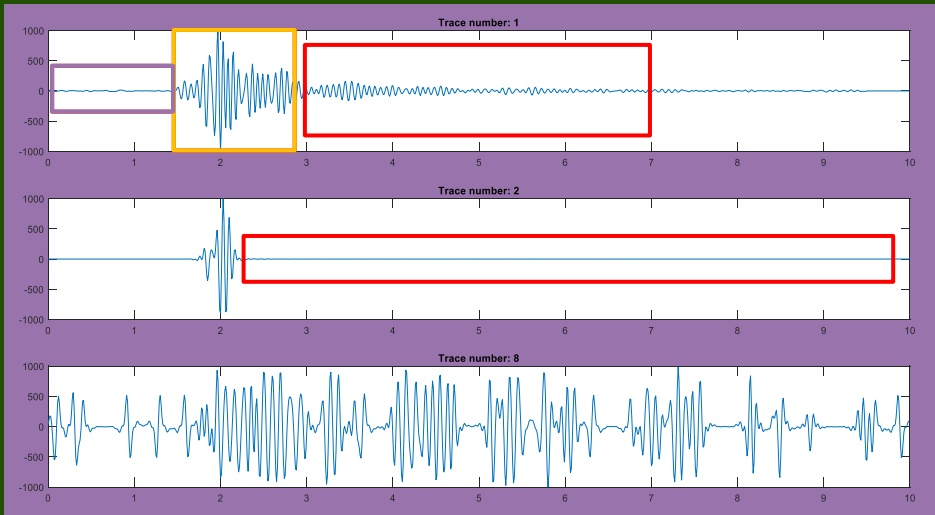


The output is generated from the contribution of all nodes of the grid to the single-station  $Q_c$  measurement

# DATA ANALYSIS



# DATA ANALYSIS



1. Zeros percentage;
2. Mean amplitude Noise windows;
3. Mean signal amplitude;
4. Signal to Noise ratio;
5. Mean amplitude Coda windows;
6. Mean amplitude max power;
7. Mean frequencies at max power;
8. Cross-correlation mean values;
9. Sum of the ampl. values  $> 500$ ;
10. Amplitude "jumps";
11. Mean Correlation coefficients;
12. Deviation Standard STA/LTA;

# DATA ANALYSIS

Zeros%	Amp Noise w	Amp Signal	S/N	Amp Coda w	MaxPow Amp	Freq MaxPow	Xcorr	Ampl>500	Jumps	CorrCoe	DevStStaLta	Num. Events
24,14472711	41,6522254	169,4206531	658,844695	86,36893258	1501055,616	11,30141498	2441546,661	49,08761031	53,3617604	0,637436169	1,12861352	20283
8,899726155	51,15679938	198,735286	35,9273832	111,5881513	1919600,057	10,81084024	3043020,852	59,4691424	65,6010488	0,558934996	0,81293642	14972
8,839893171	45,3949275	195,5547233	37,0140766	105,7499993	1778461,021	11,00276994	2880608,398	53,41411675	62,3985658	0,608990486	0,85451556	13105
8,914667511	18,37416775	168,6745146	40,5085317	80,80920191	1197581,724	11,78	2140024,209	30,20443319	48,1508695	0,798962086	1,03212687	7895
8,595400222	18,07422623	169,4120495	35,7345383	81,03120393	1189359,401	11,83091996	2142433,739	29,16050584	48,3483346	0,800404036	1,02829843	7197

Iterative selection on the basis of  $\text{CorrCoe} \leq 0.6$

20283 → 7197

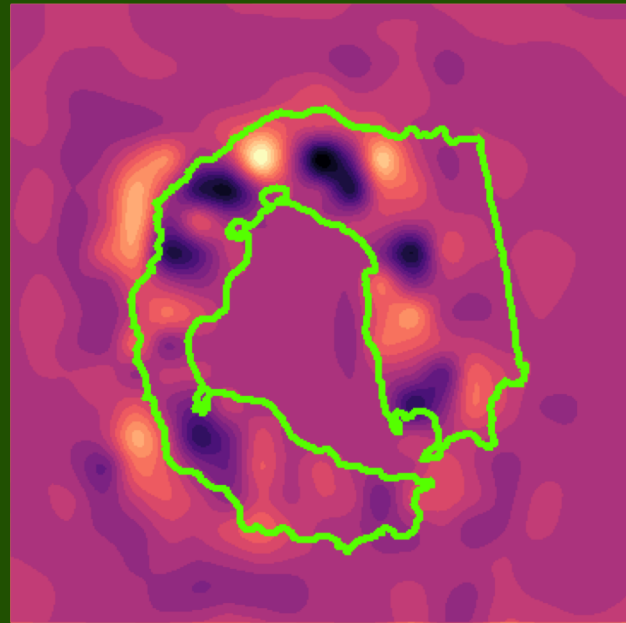
Filtering in five frequency bands, centered at 6 , 9 , 12 , 15 and 18 Hz;  
4 seconds of Coda windows (starting from the main peak);  
Grid resolution of 1 and 2 km.



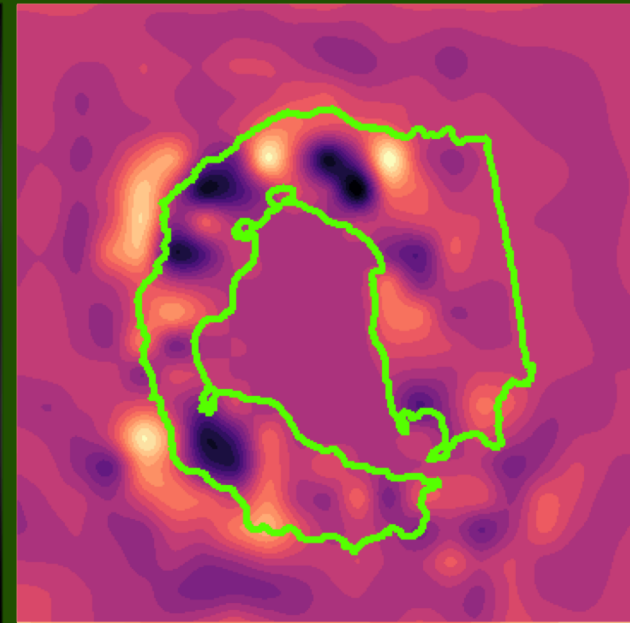
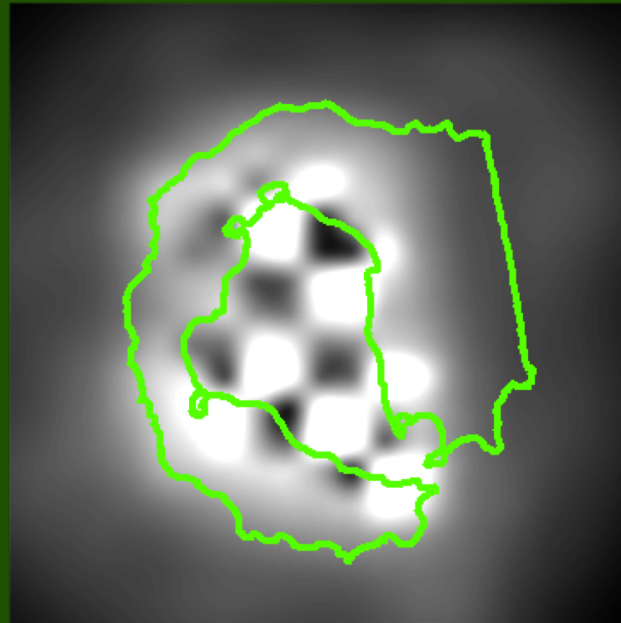
# RESULTS

(1km resolution)

Original (lots of noise)



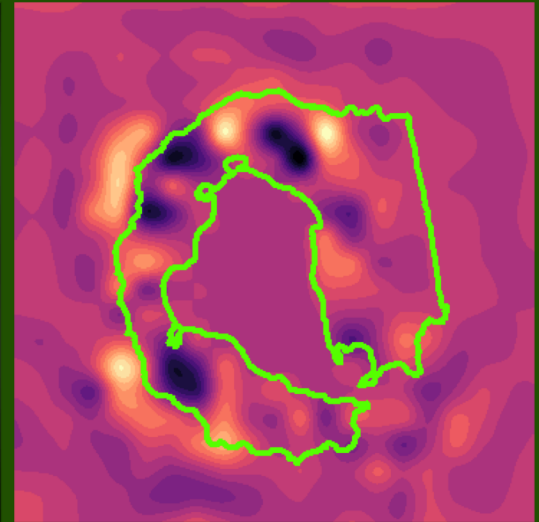
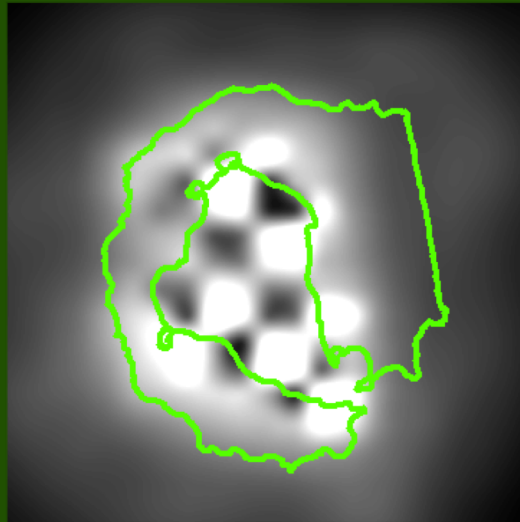
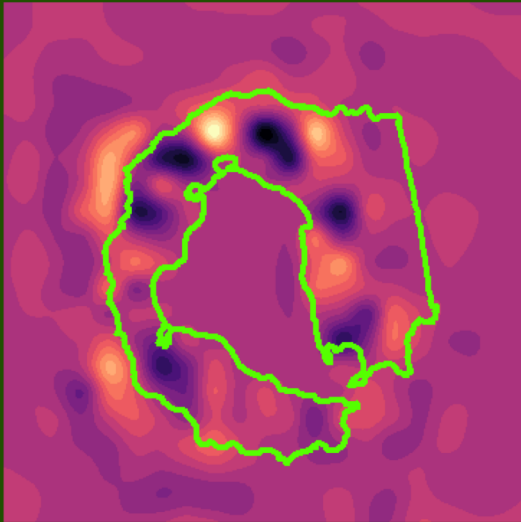
6 Hz



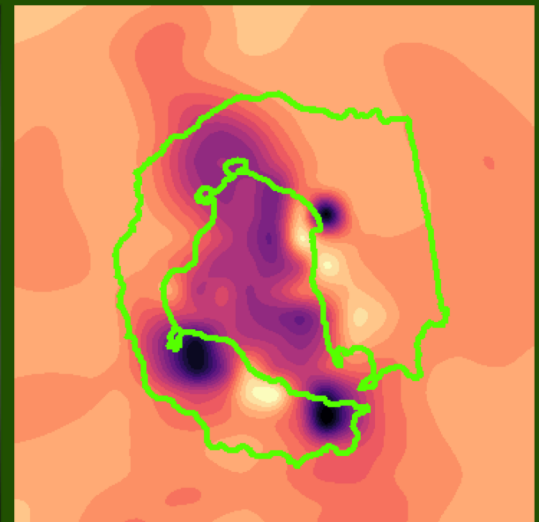
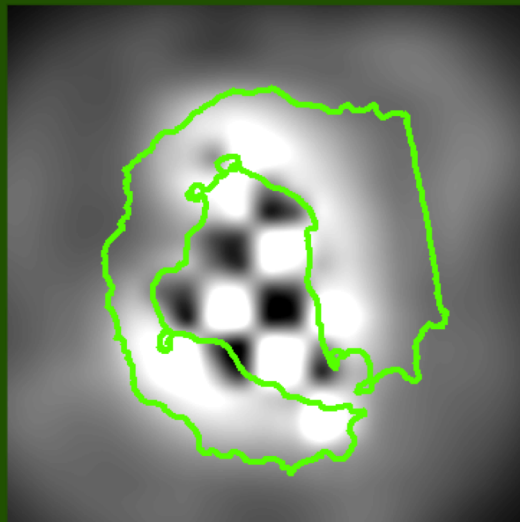
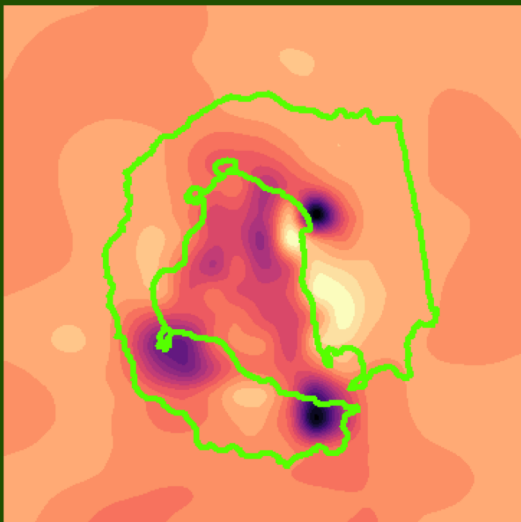
15 Hz

# RESULTS (1km res.)

Original dataset



Iteration: 4

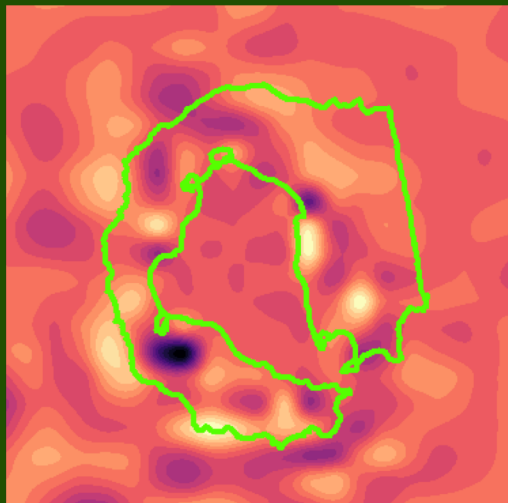
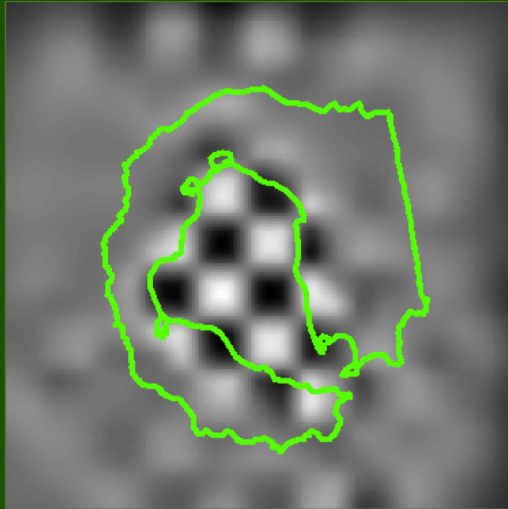


6 Hz

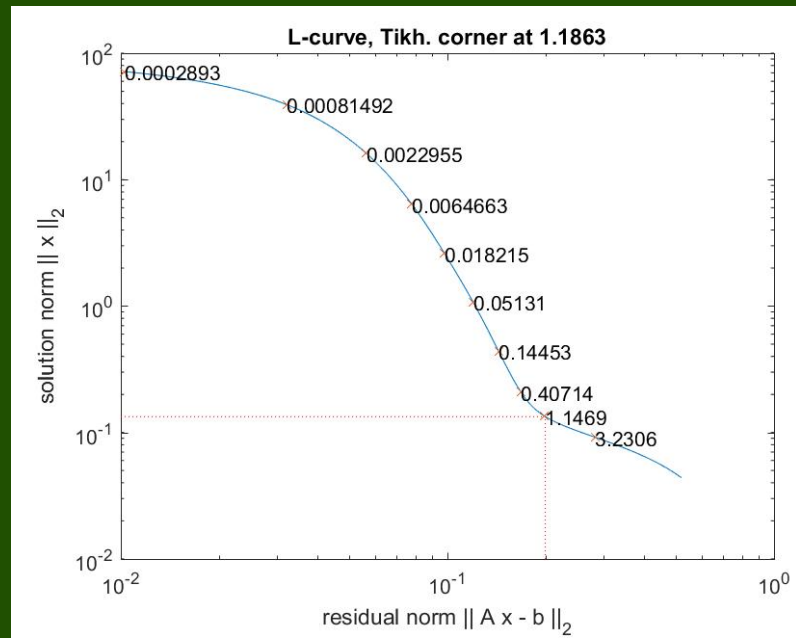
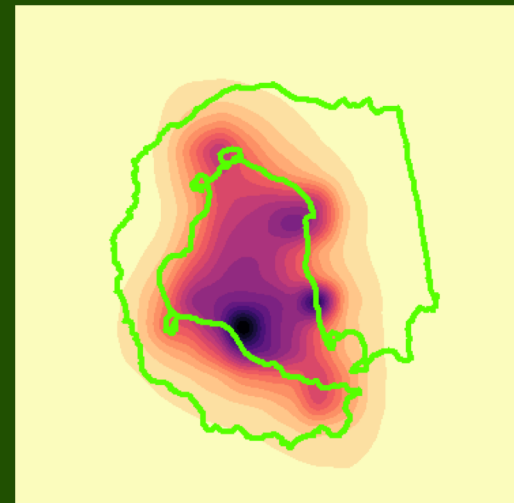
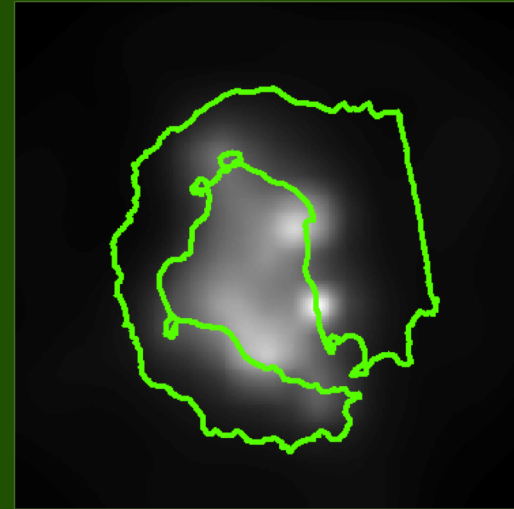
15 Hz

# Tikhonov reg. (1km res. – 15 Hz)

0.118



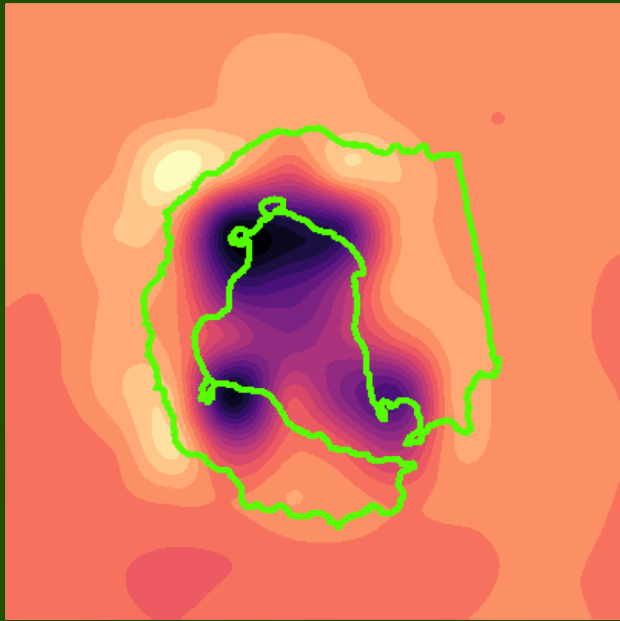
11.8



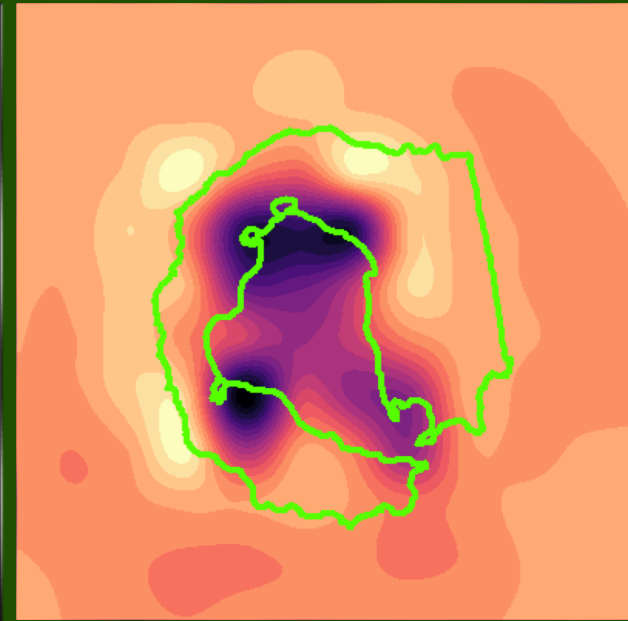
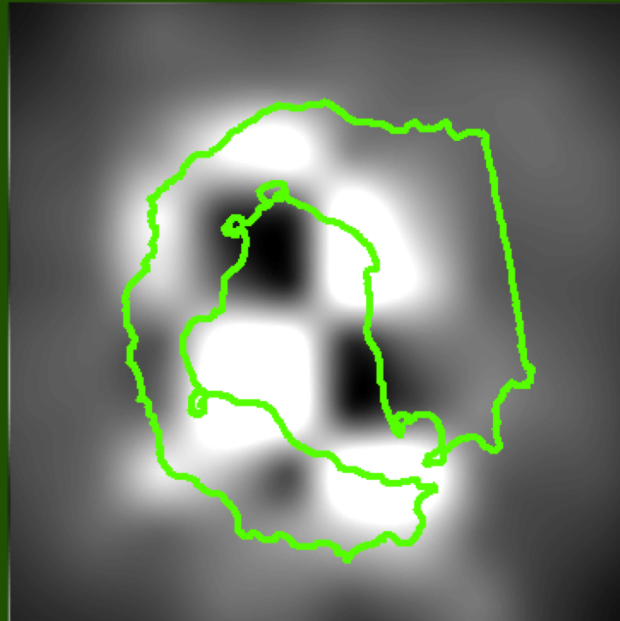
# RESULTS

(2km resolution)

Iteration 1 (last series)



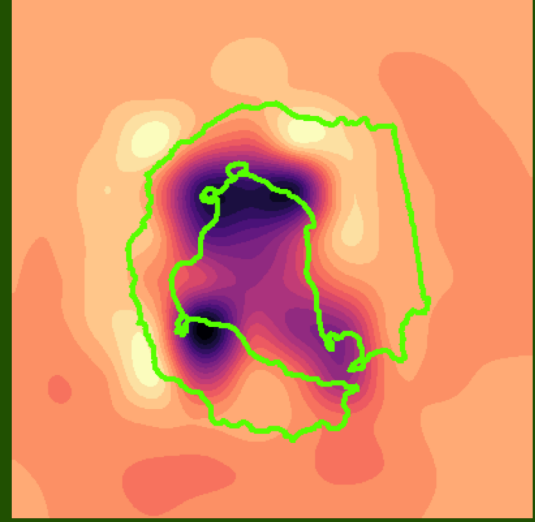
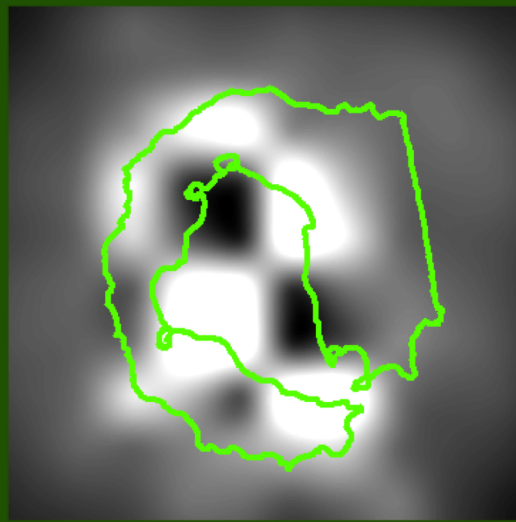
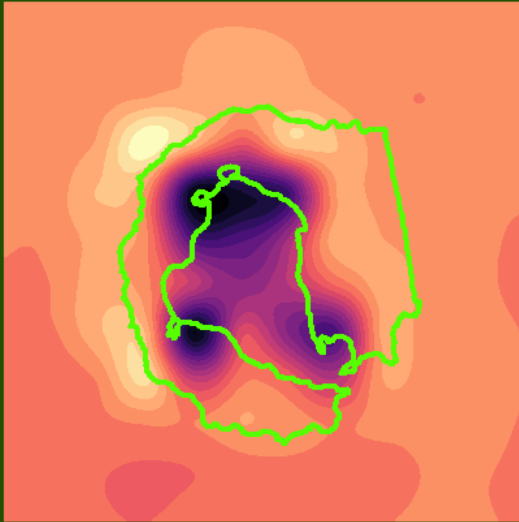
6 Hz



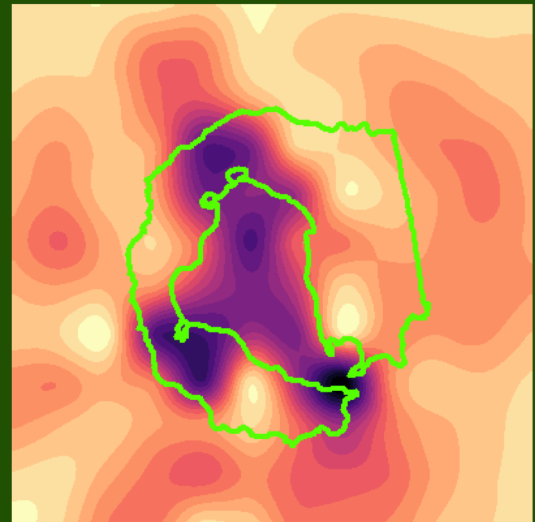
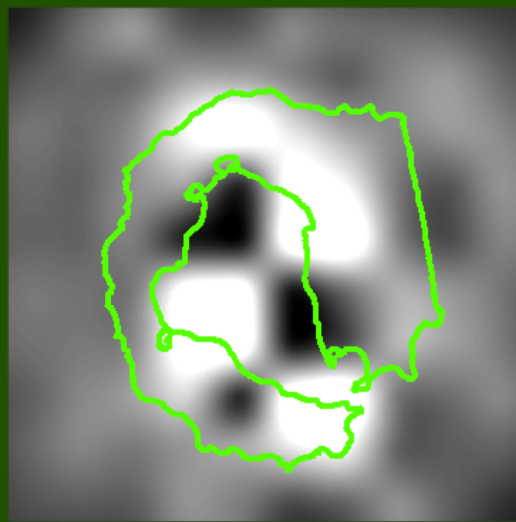
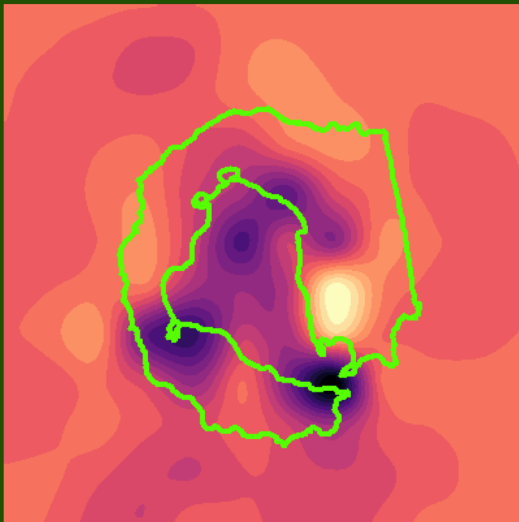
15 Hz

# RESULTS (2km res.)

Original dataset



Iteration: 4

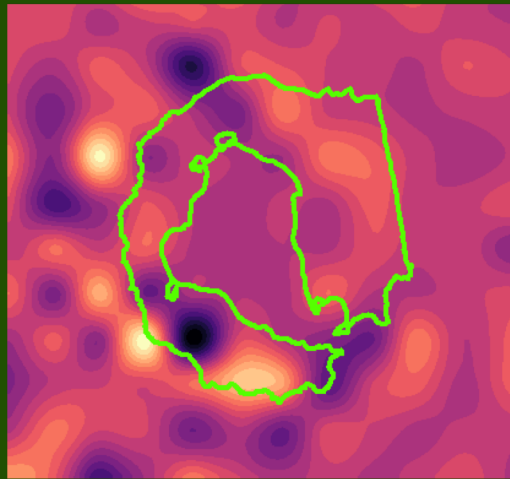
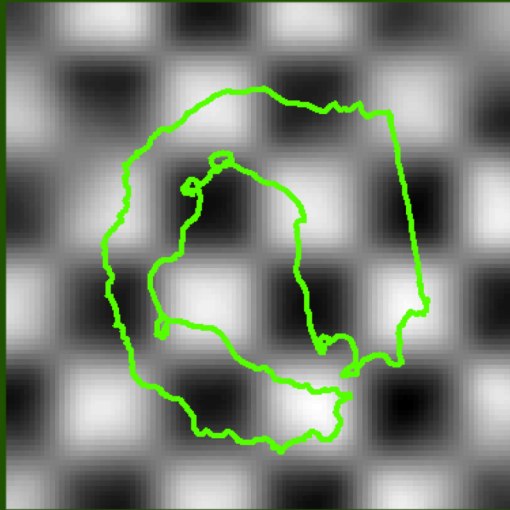


6 Hz

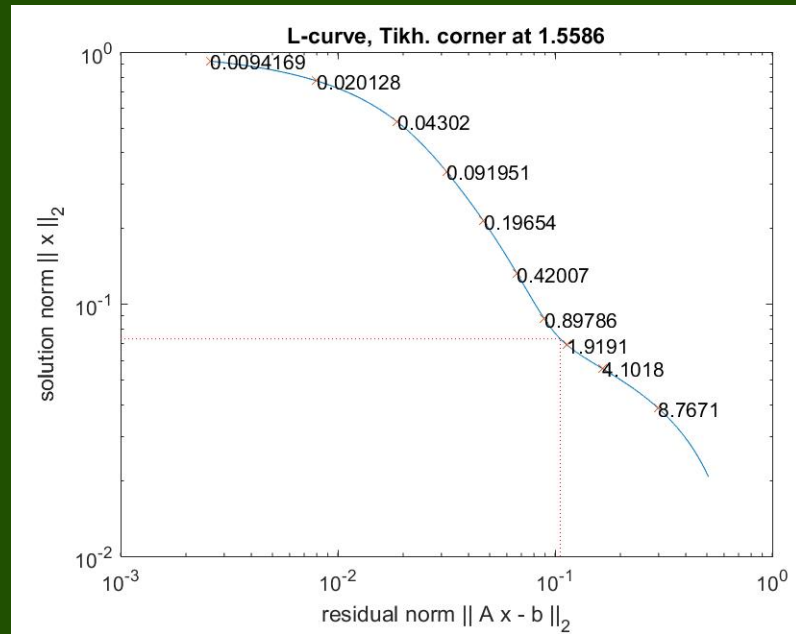
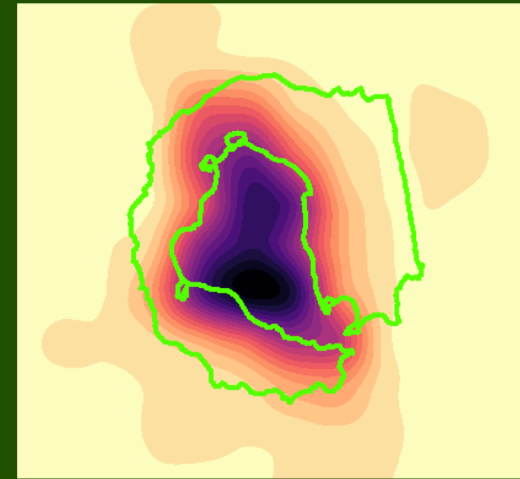
15 Hz

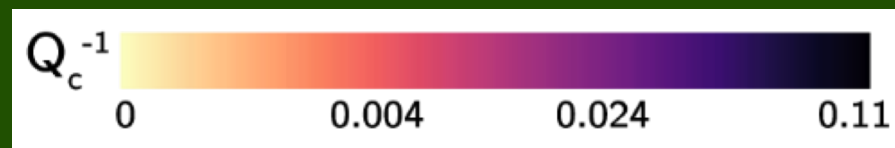
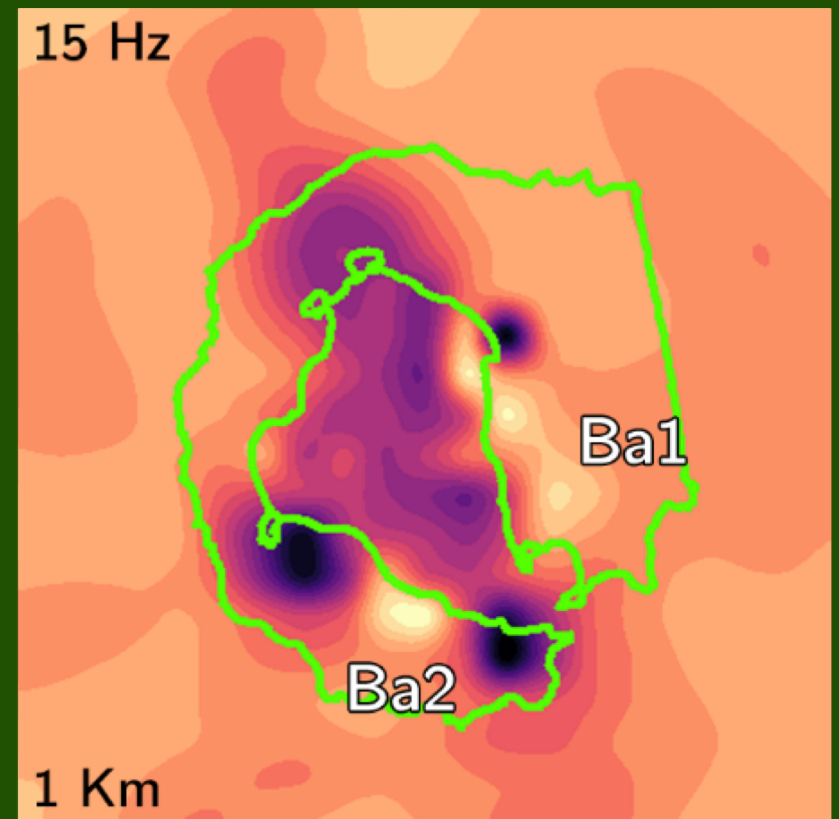
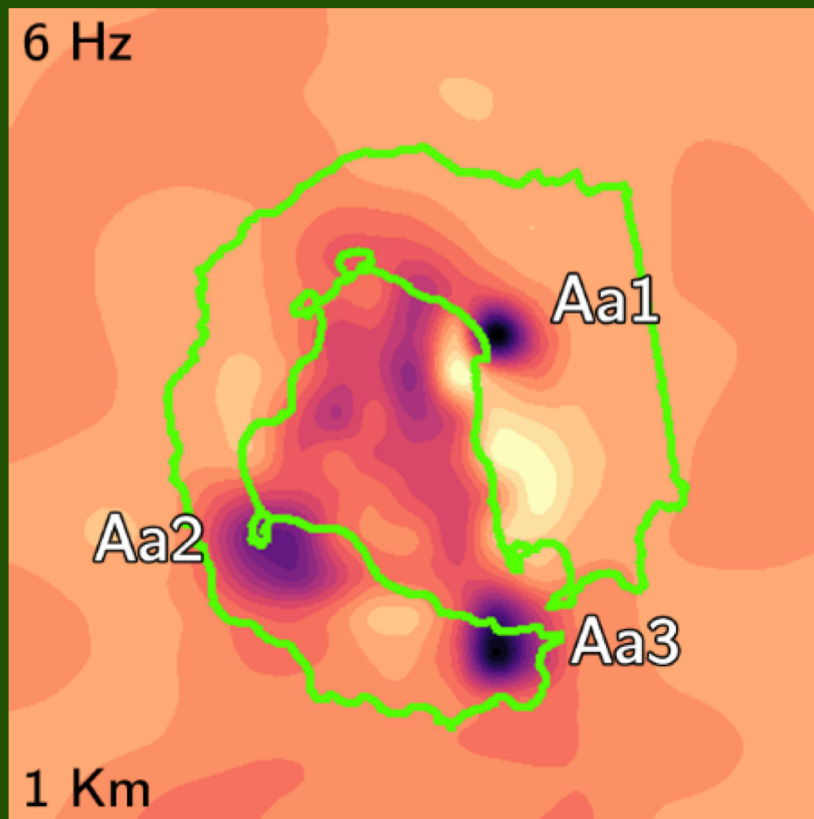
# Tikhonov reg. (2km res. – 15 Hz)

0.155



15.5

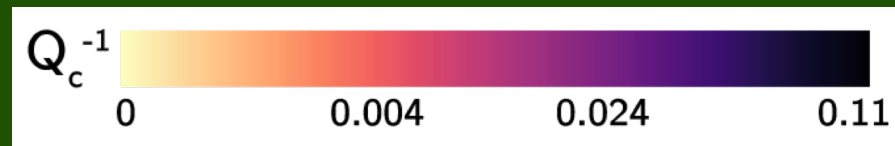
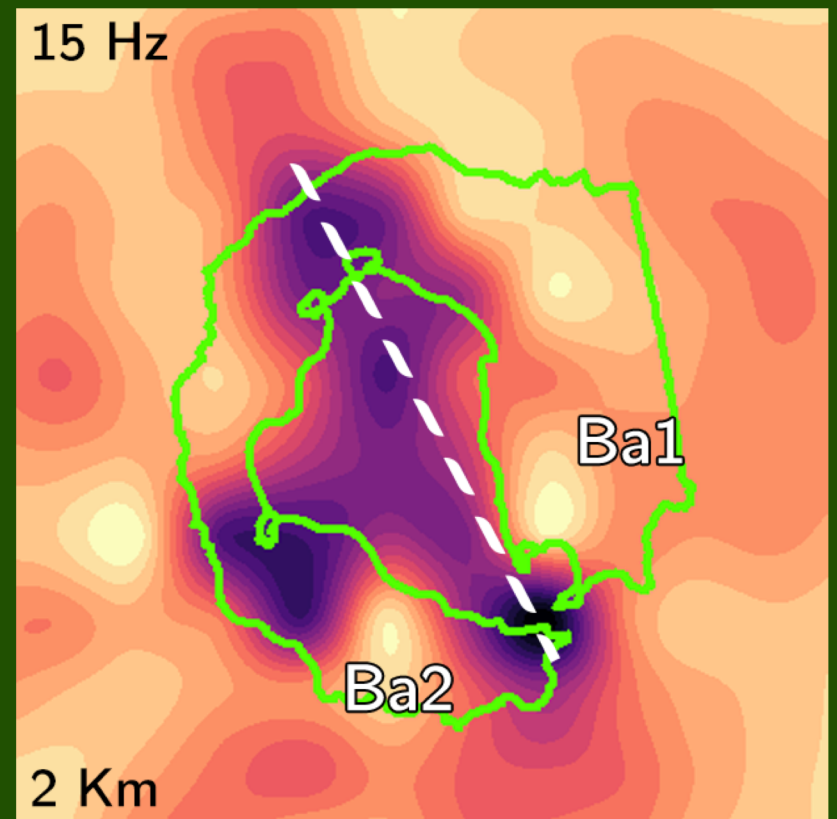
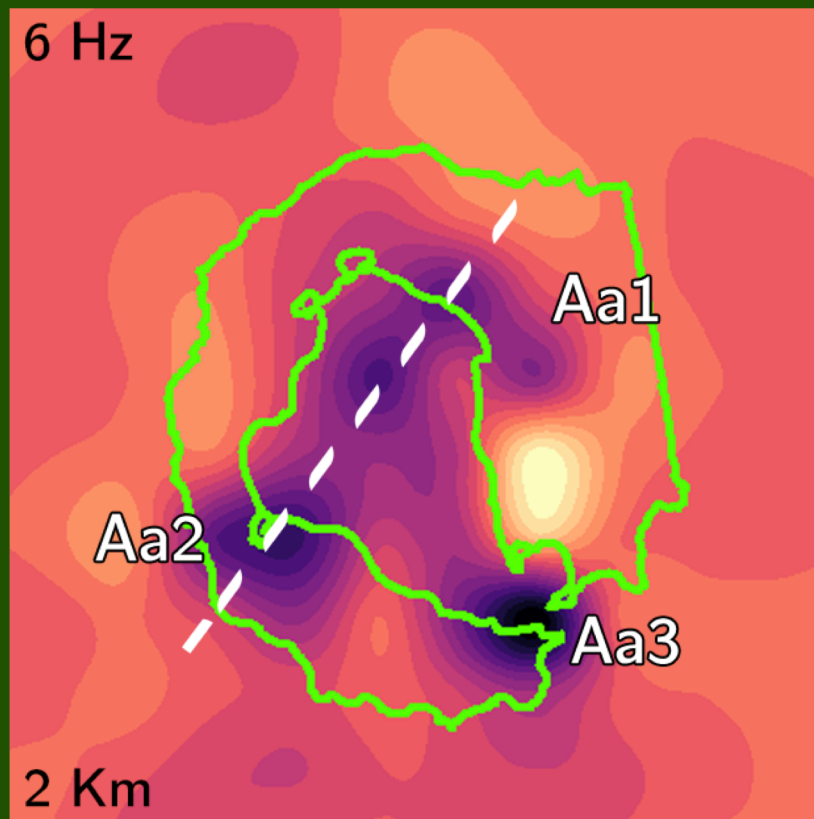




**Aa# = High attenuation**  
**Ba# = Low attenuation**

We consider the high attenuation areas as rocks characterized by hot fluids or magmatic batches and the low attenuation ones as cooling magmatic body.





**Aa# = High attenuation**  
**Ba# = Low attenuation**

We consider the high attenuation areas as rocks characterized by hot fluids or magmatic batches and the low attenuation ones as cooling magmatic body.

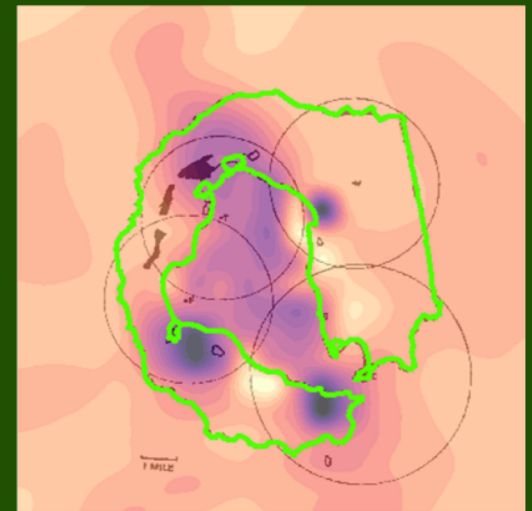
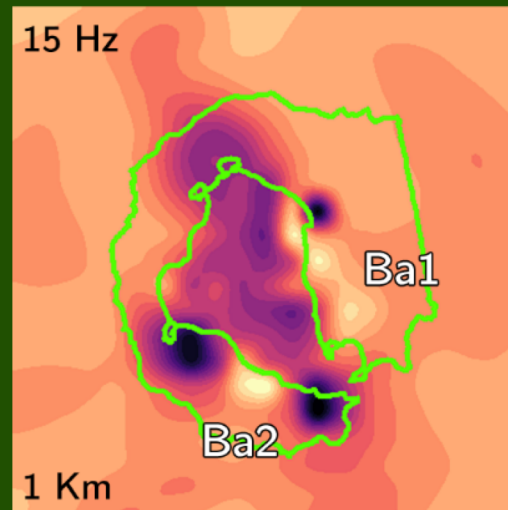
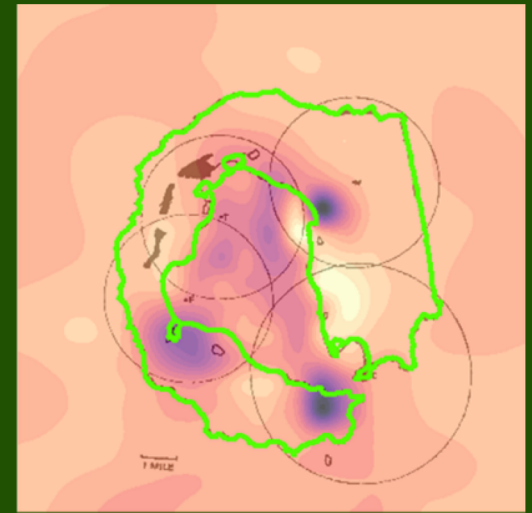
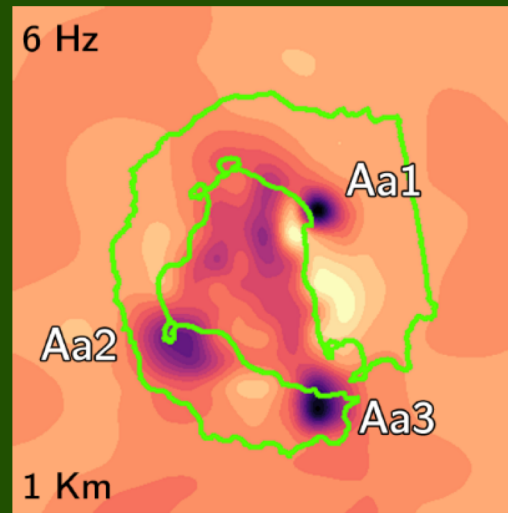
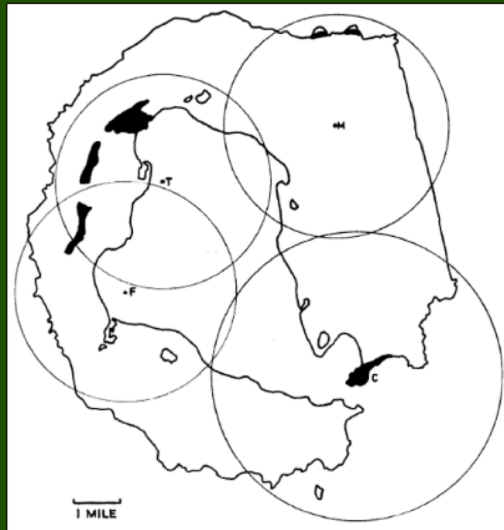


# DISCUSSIONS

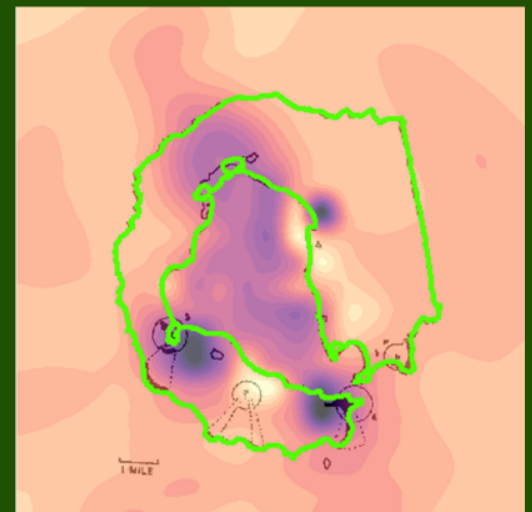
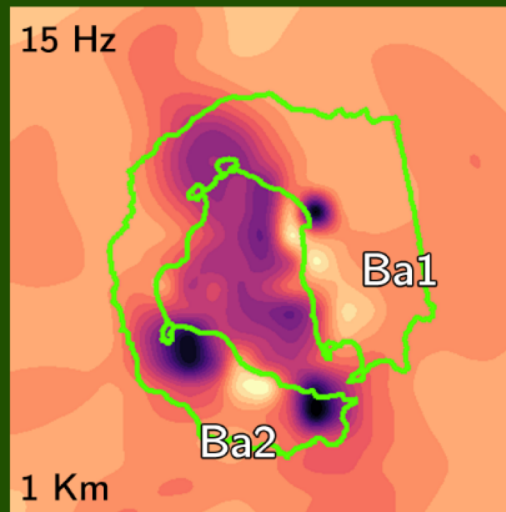
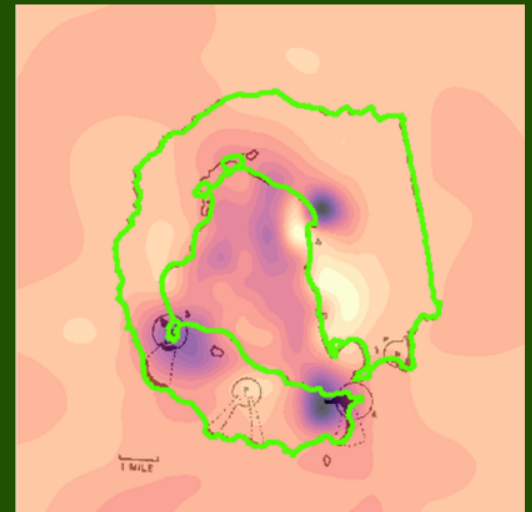
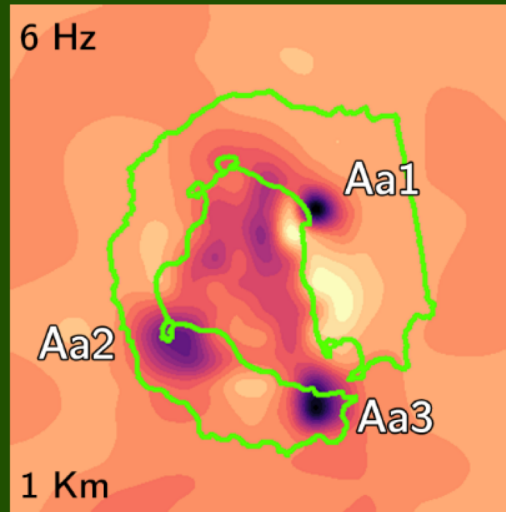
## Comparison with previous studies:

- Geology
- Tectonics
- Geochemistry
- Geophysics
- Volcanic hazard

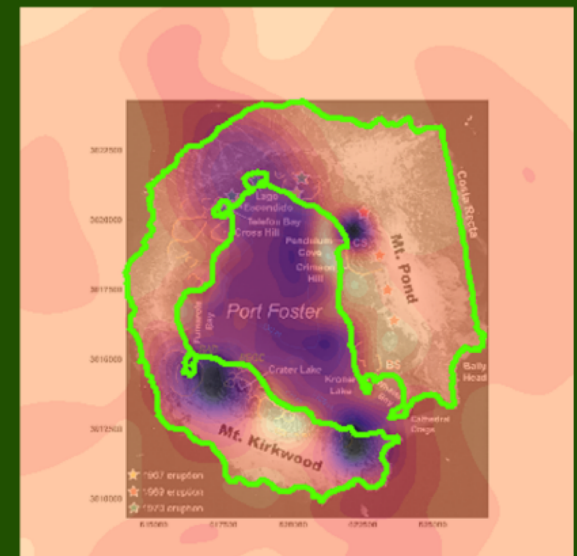
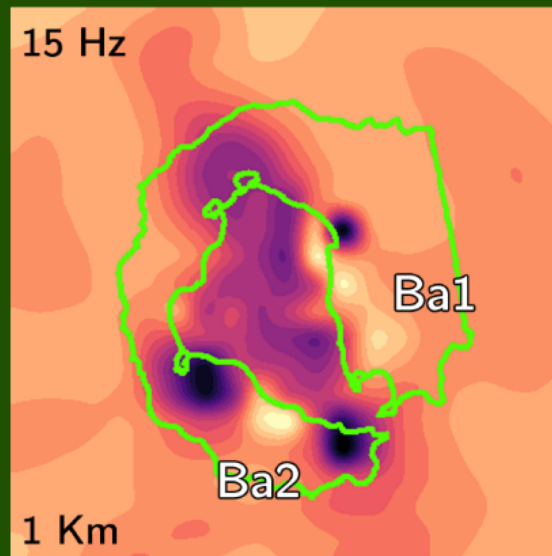
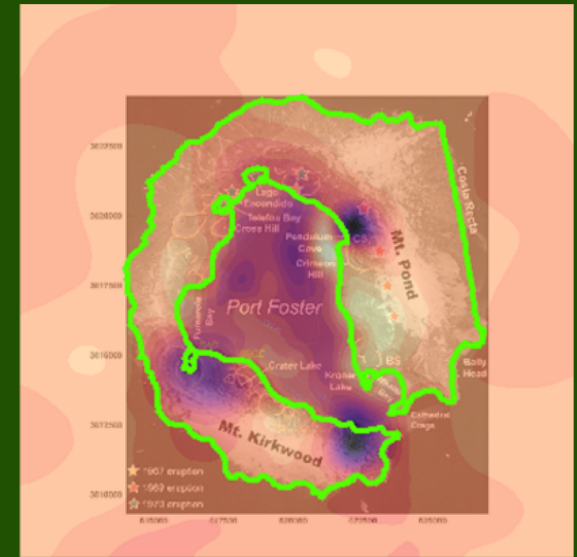
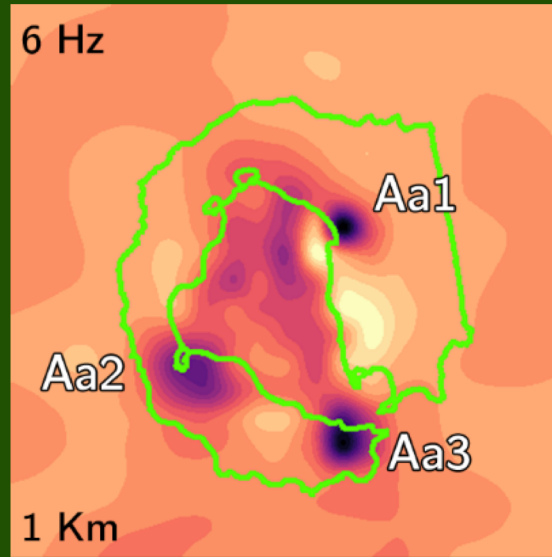
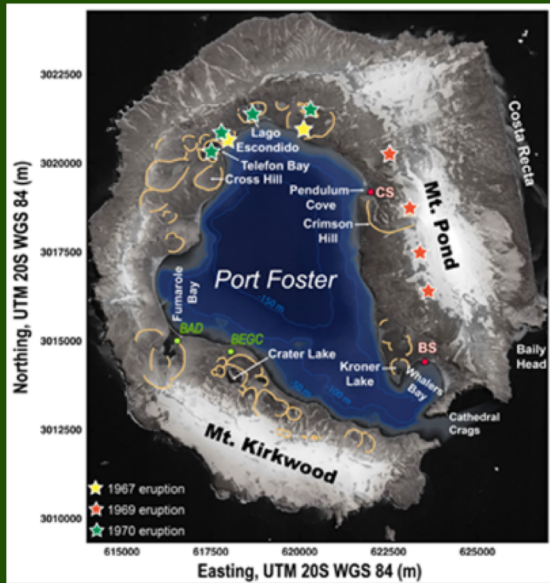
# Comparison with previous geological studies



Hawkes et al. 1961 – Fig. 3  
Volcanic centres of the «pre-caldera» group.

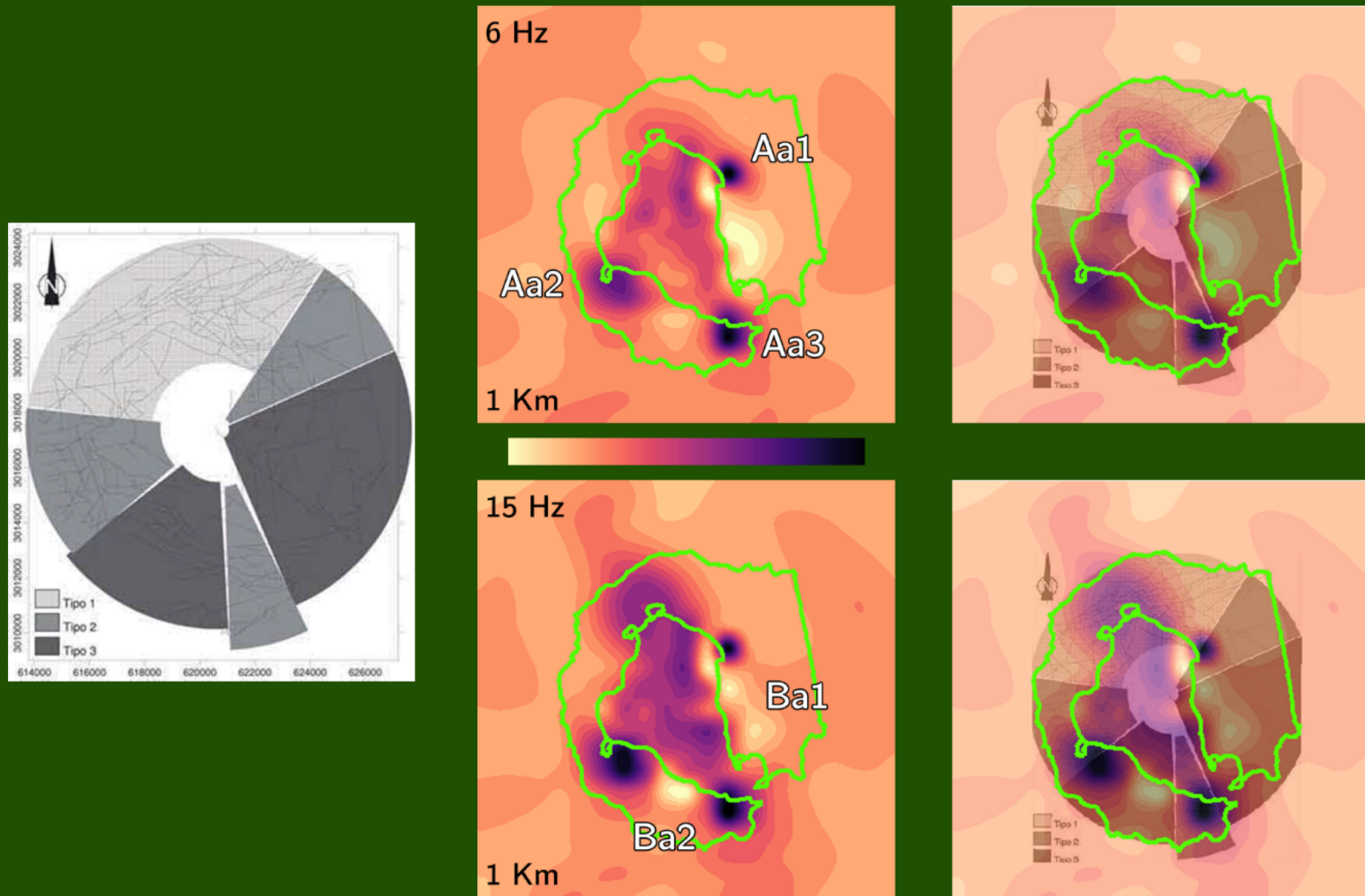


Hawkes et al. 1961 – Fig. 6  
Volcanic centres of the «Neptune bellow» group.



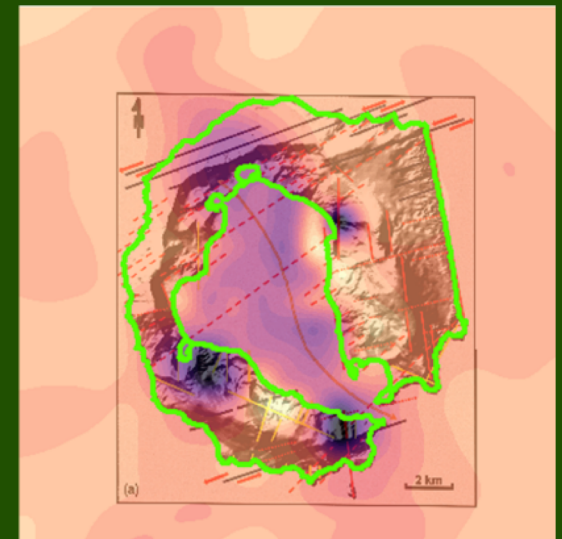
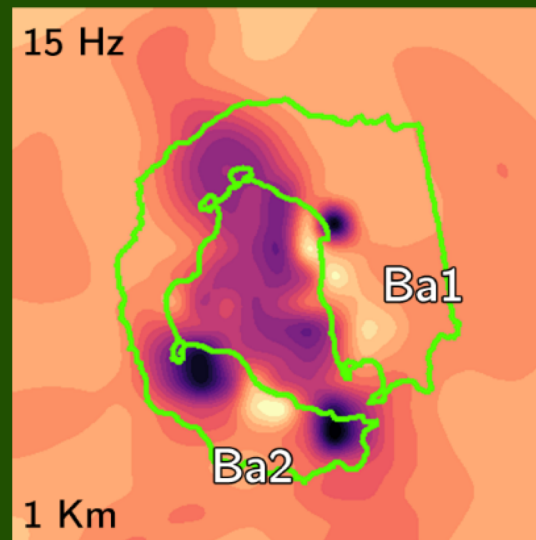
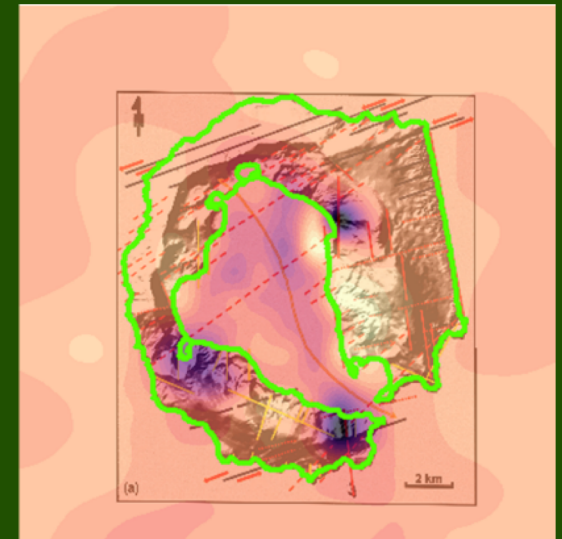
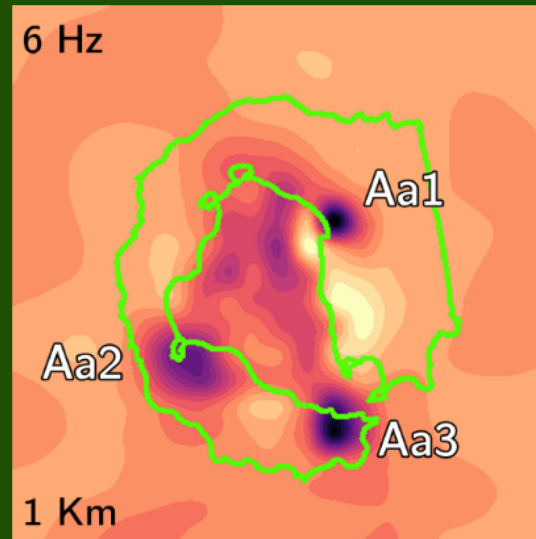
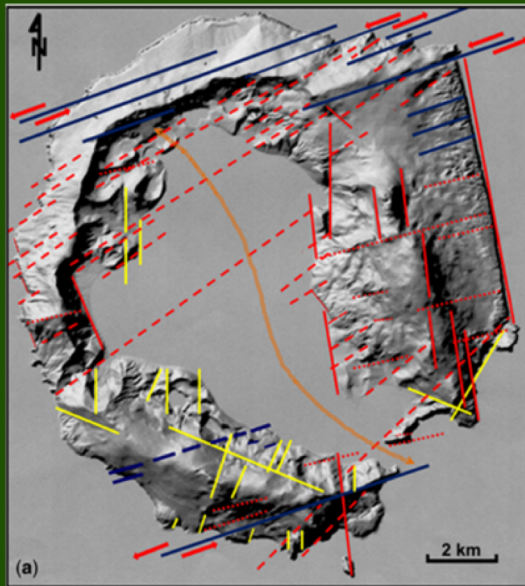
Geyer et al. 2019 – Fig. 1B  
Location of the last eruptive centres

# Comparison with previous tectonics studies

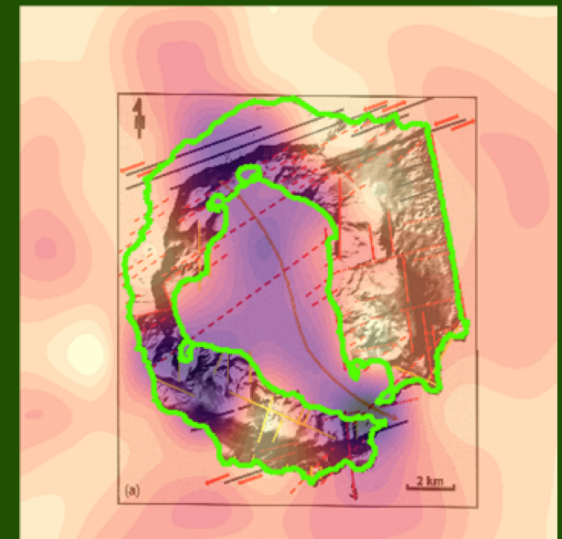
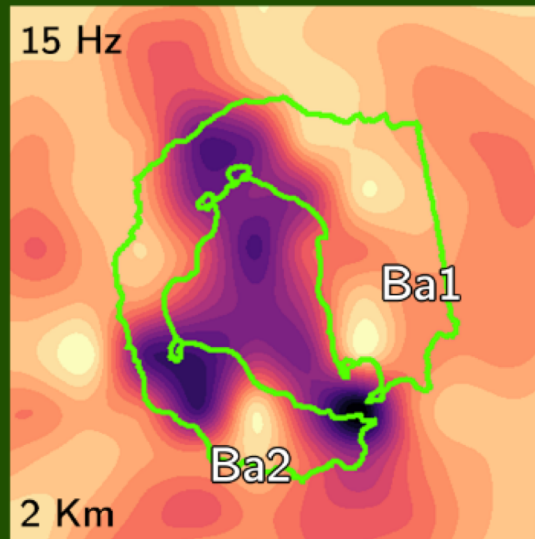
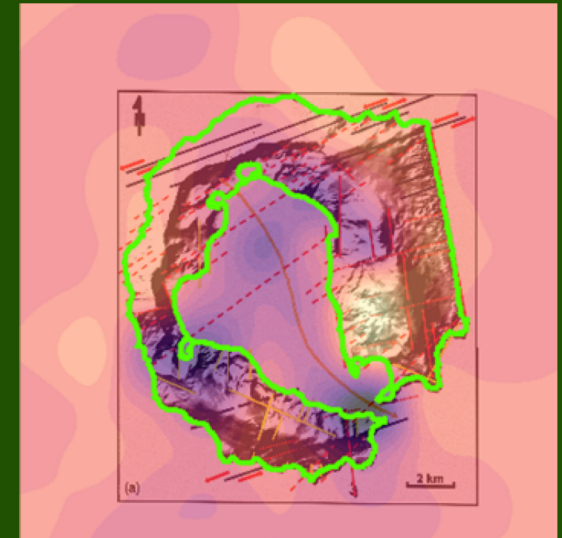
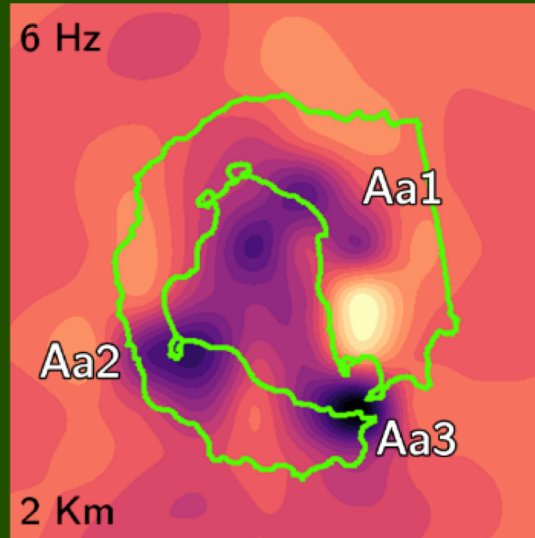
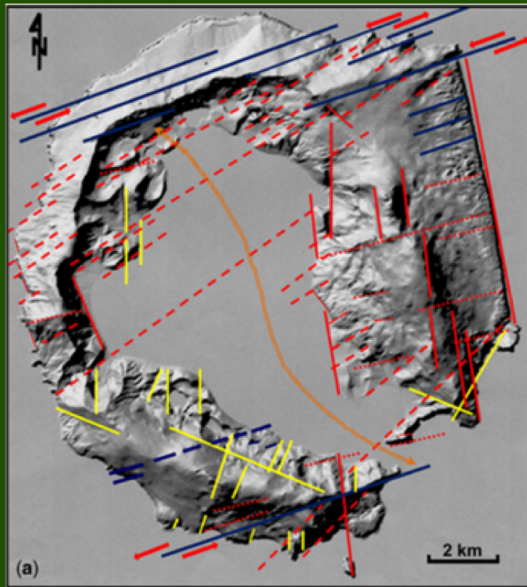


Paredes et al. 2006 – Fig. 4  
Spatial distribution of morpholineaments and tectonic zoning.



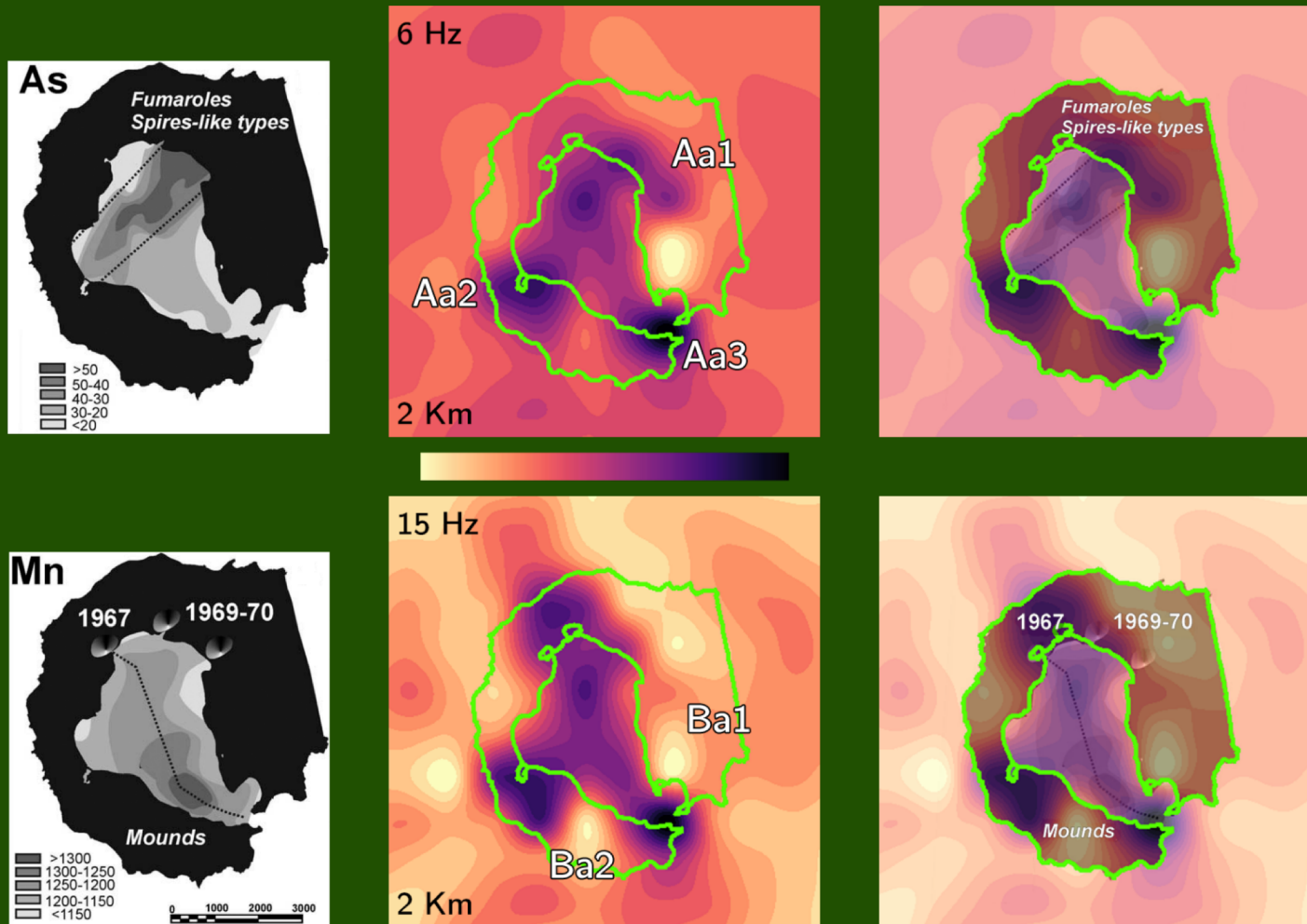


Lopes et al. 2015 – Fig. 4  
Main structural alignments that control the morphology



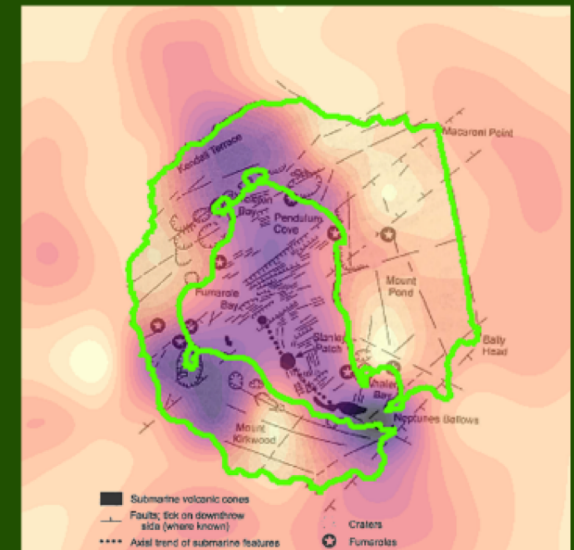
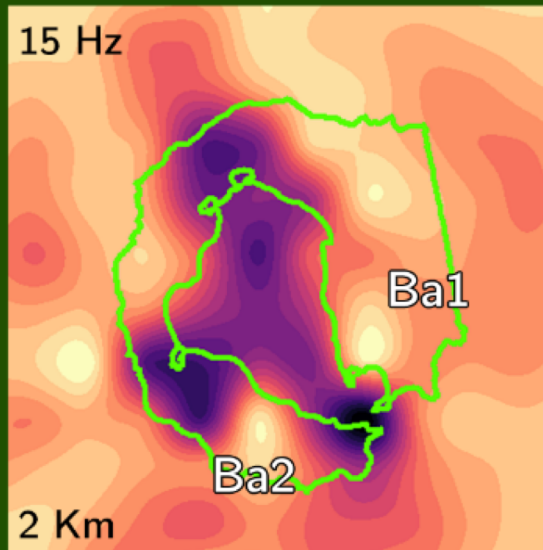
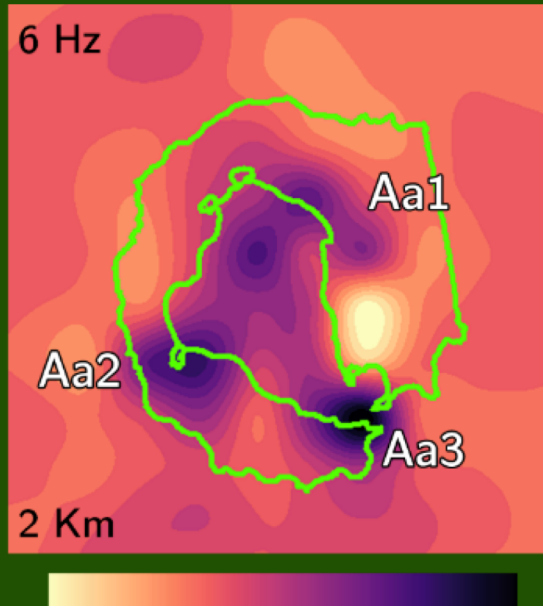
Lopes et al. 2015 – Fig. 4  
Main structural alignments that control the morphology

# Comparison with previous geochemical studies



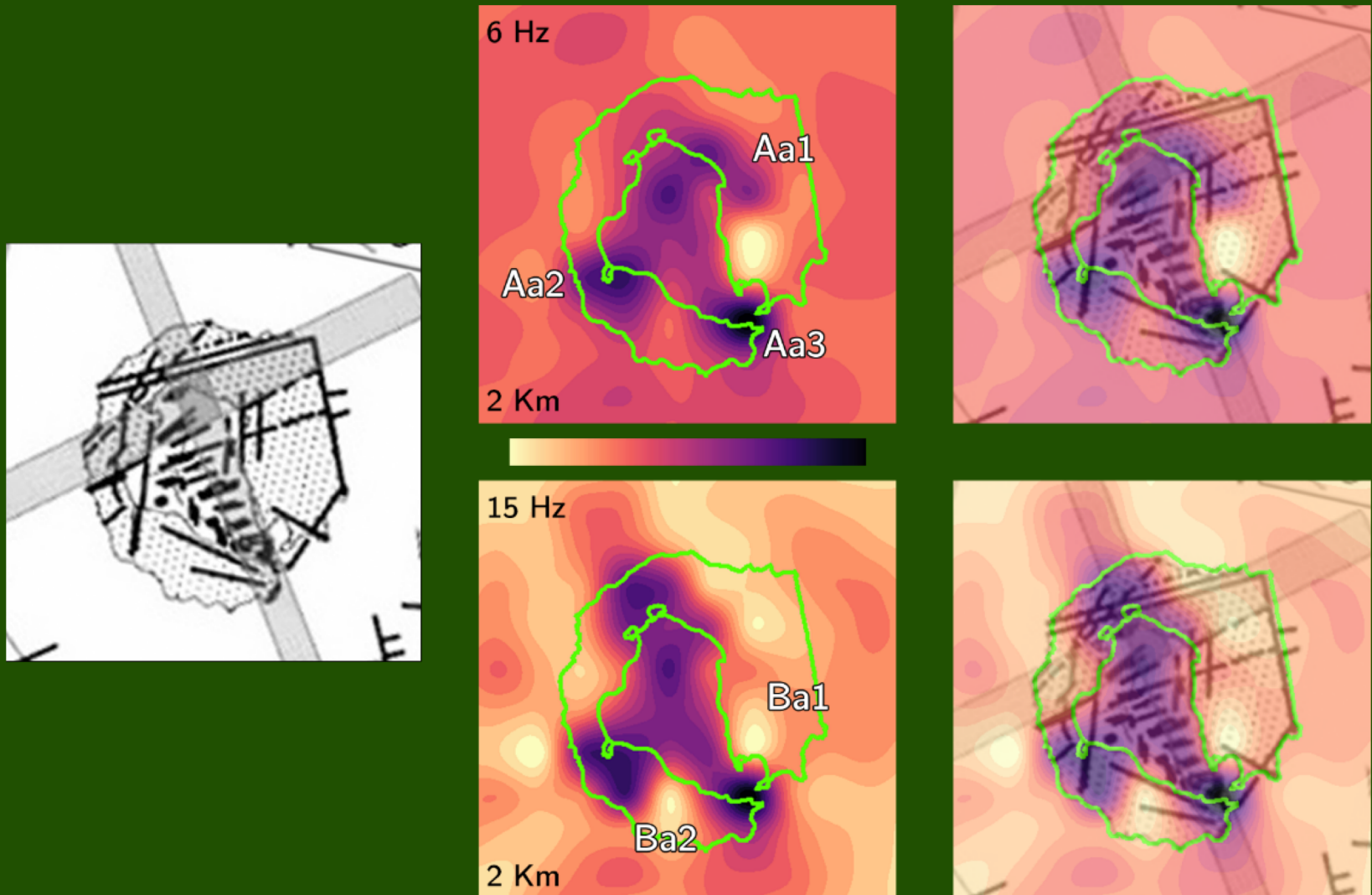
Somoza et al. 2004 – Fig. 8  
As and Mn distribution



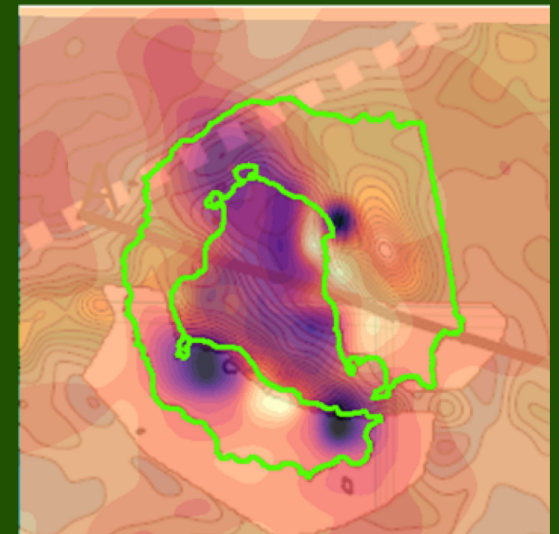
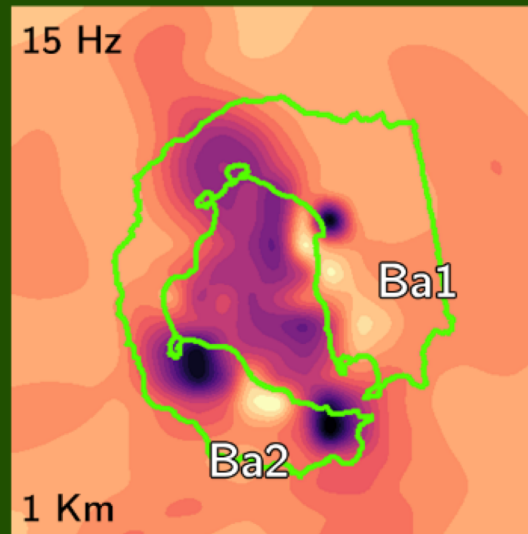
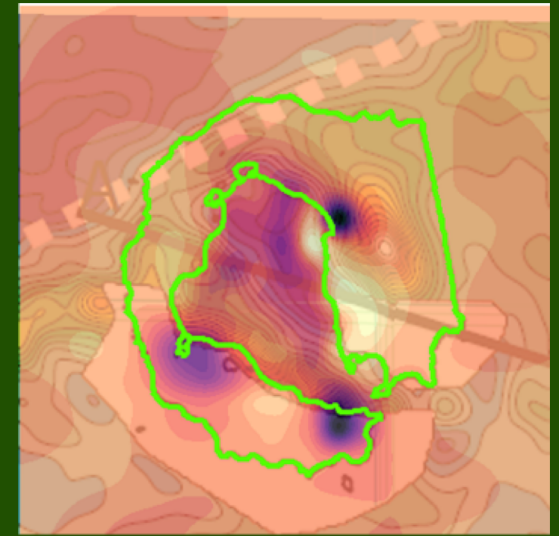
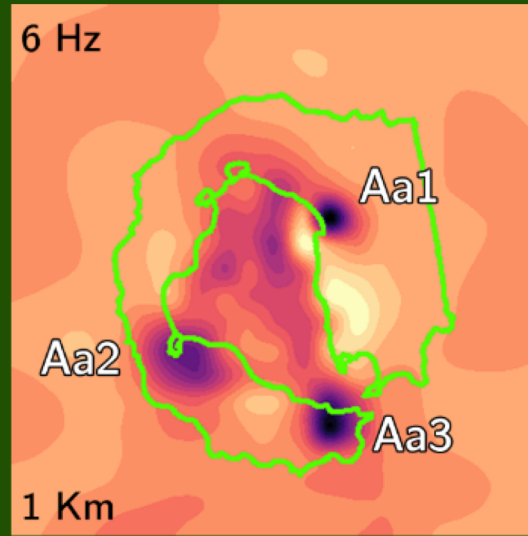
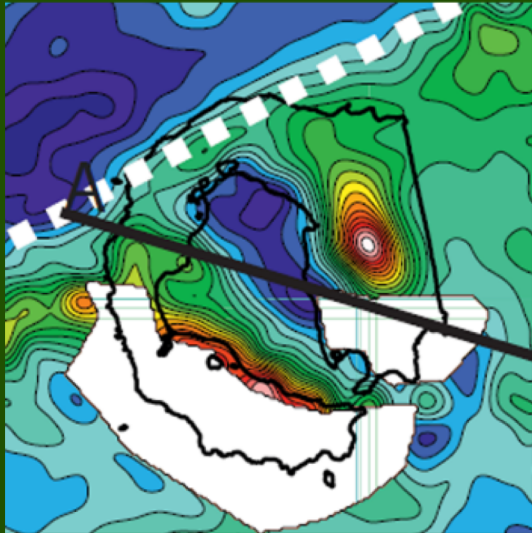


Rey et al. 2002 – Fig. 5.5  
 Distribution of fumarolic areas.

# Comparison with previous geophysical studies

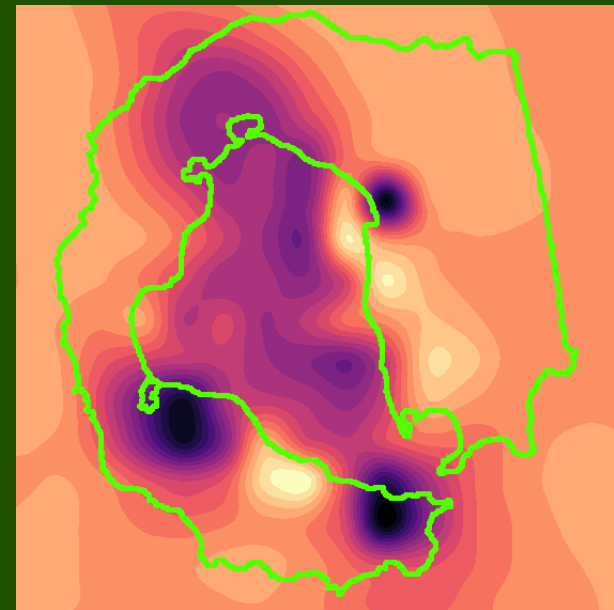
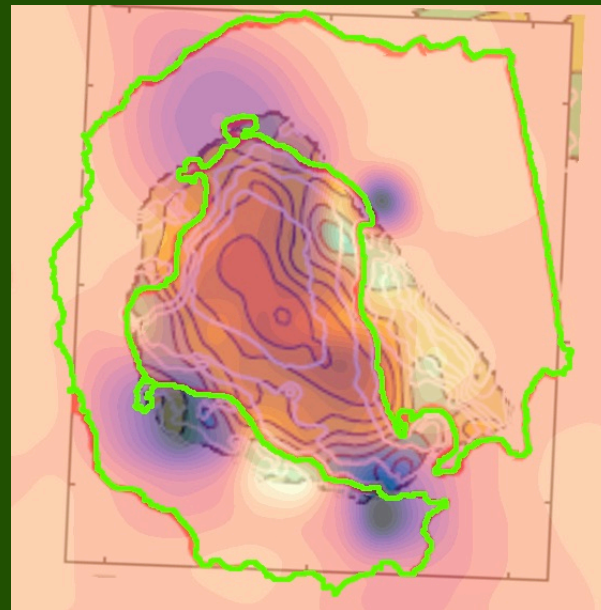
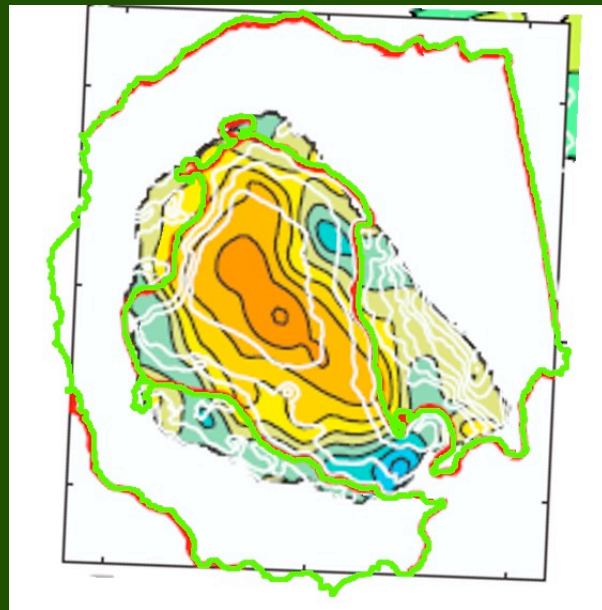


Berrocso et al. 2008 – Fig. 10  
Deformation processes during 91/00 (NNW-SSE) and 02/03 (NE-SW)



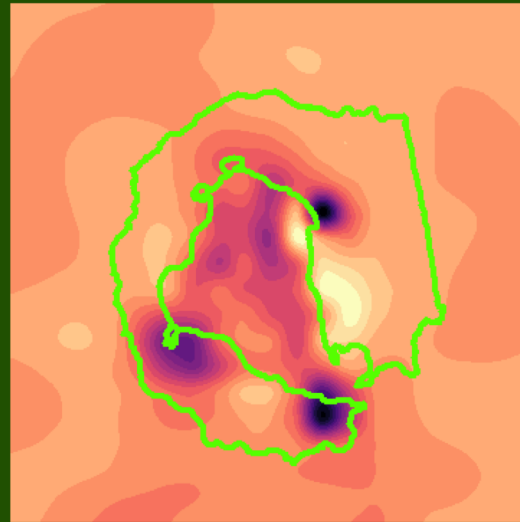
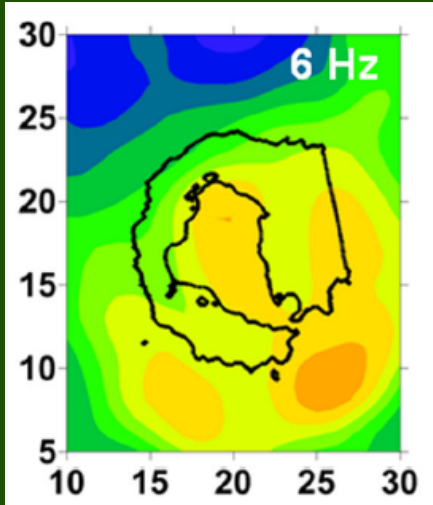
Catalan et al. 2014 – Fig. 4a  
Positive magnetic anomaly close by the Low Attenuation area (Ba1)



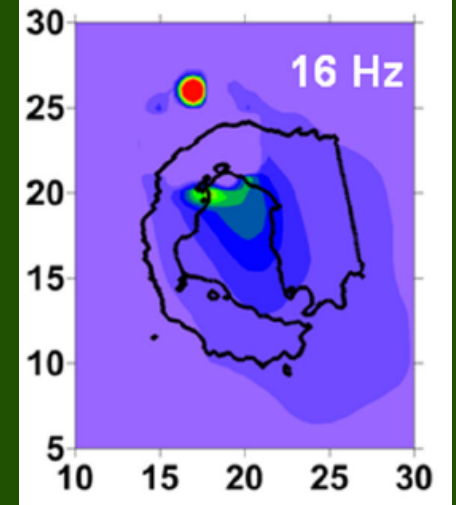
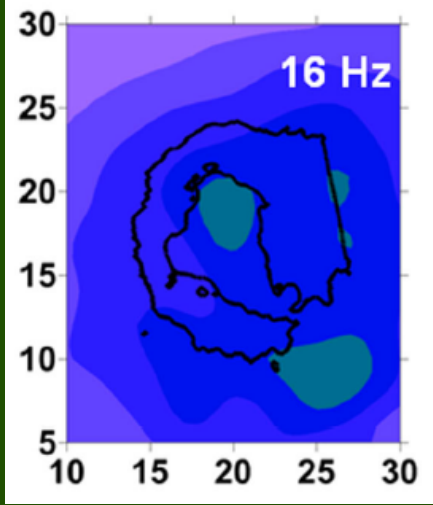
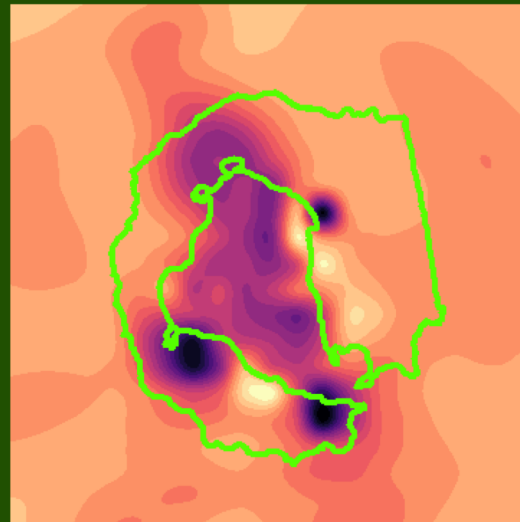
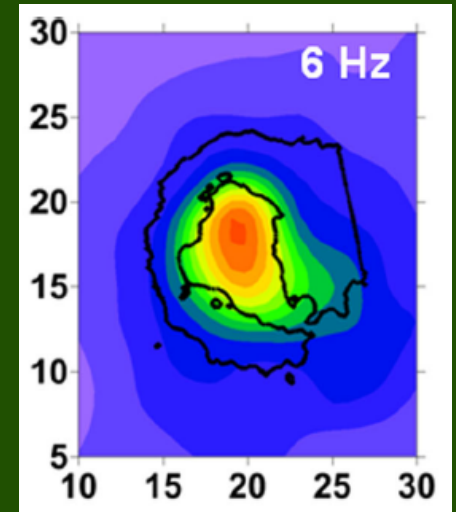


Zandomeneghi et al. 2009 – Fig. 6  
Velocity tomography model (1km depth)

Qi

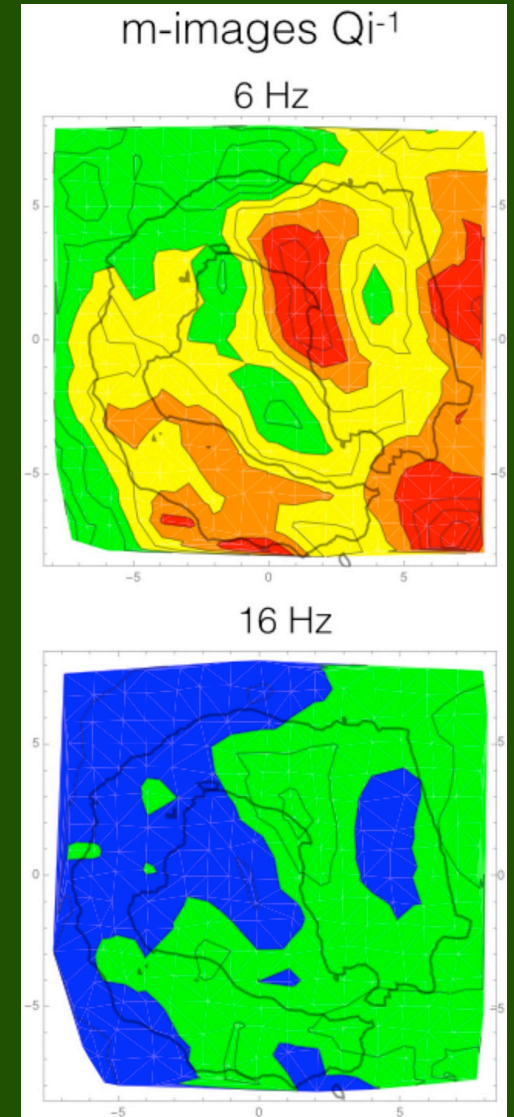
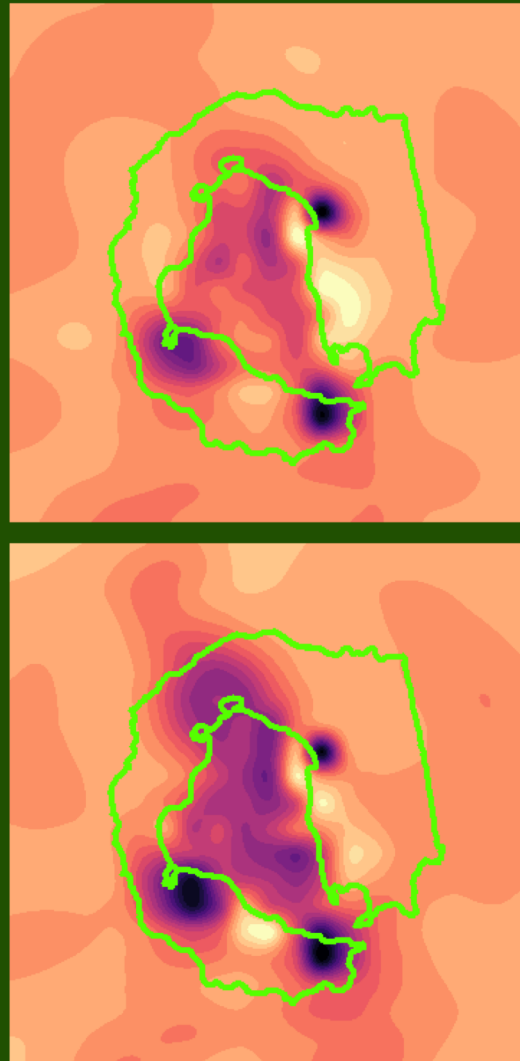
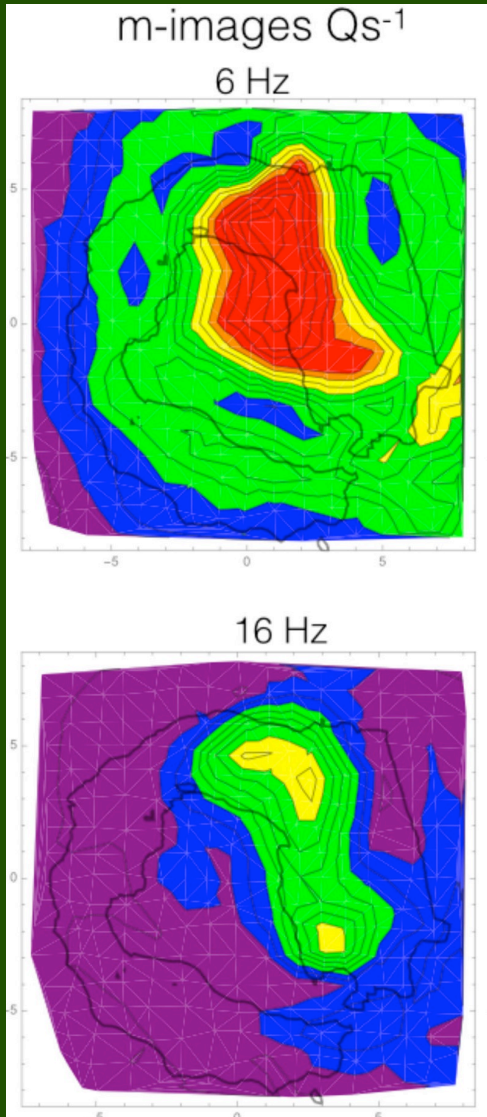


Qs



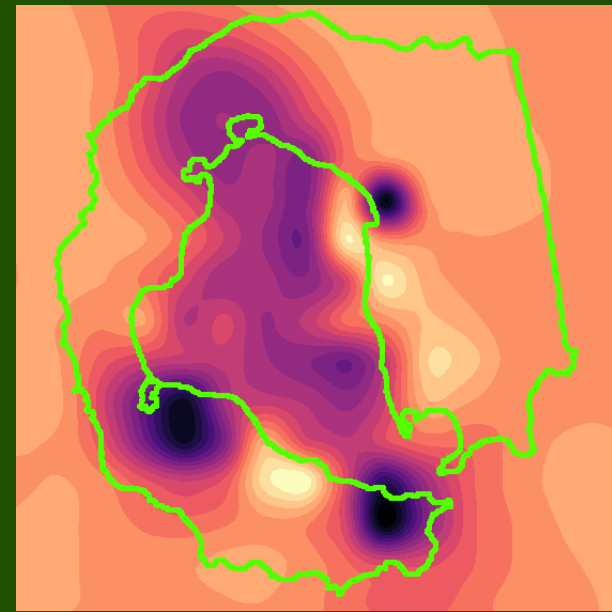
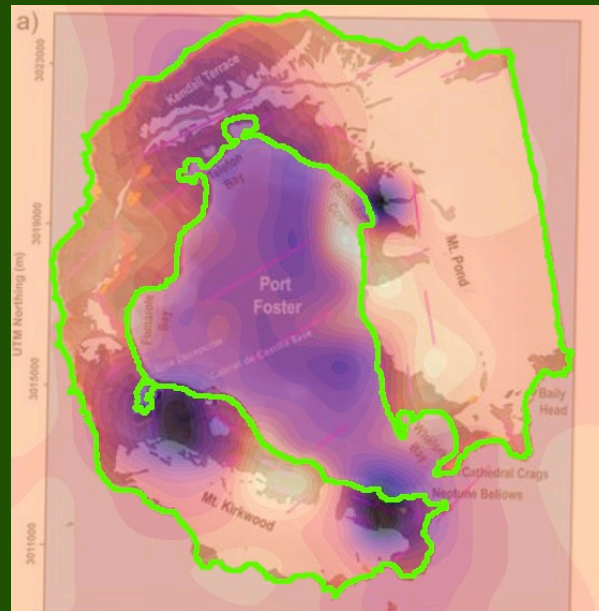
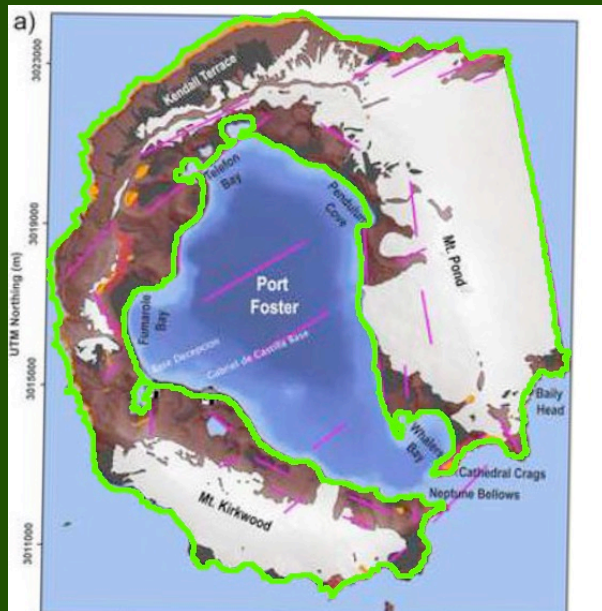
Prudencio et al. 2013

The high attenuation areas (yellow to red) matches our anomalies.



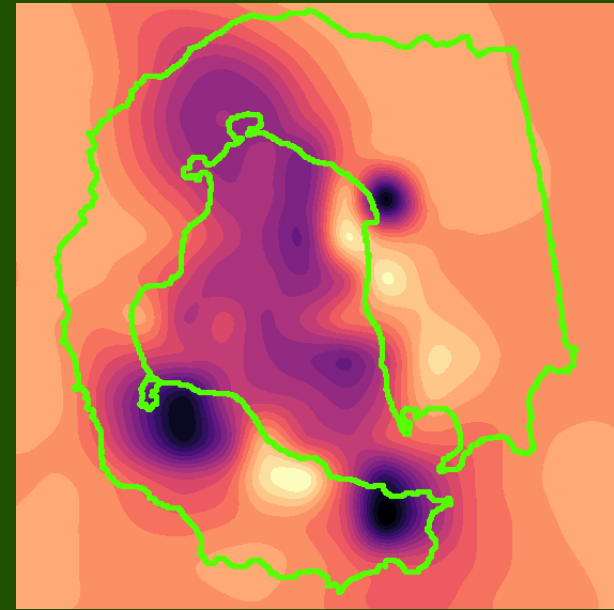
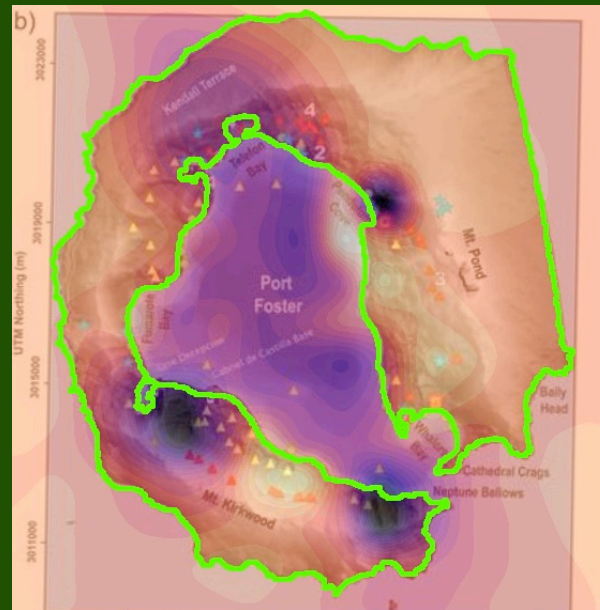
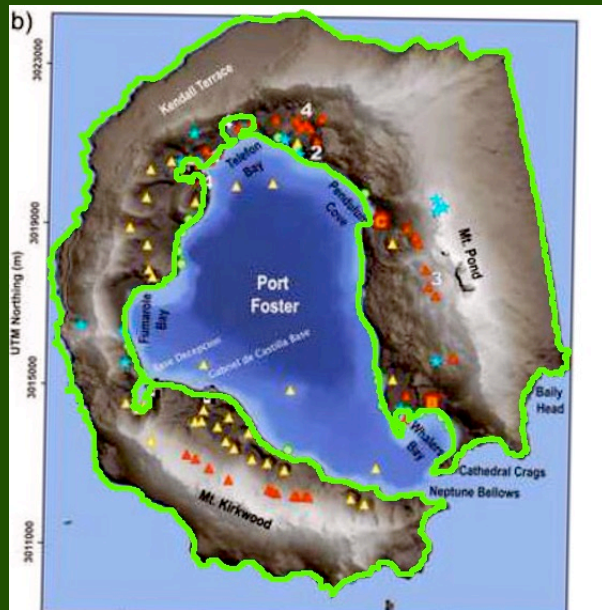
Del Pezzo et al. 2016  
Middle-point weighting functions to the single-station measurements

# Comparison with previous volcanic hazard studies



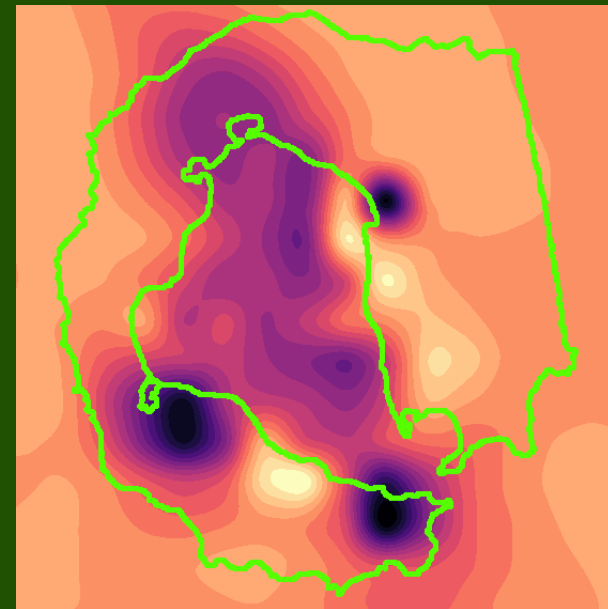
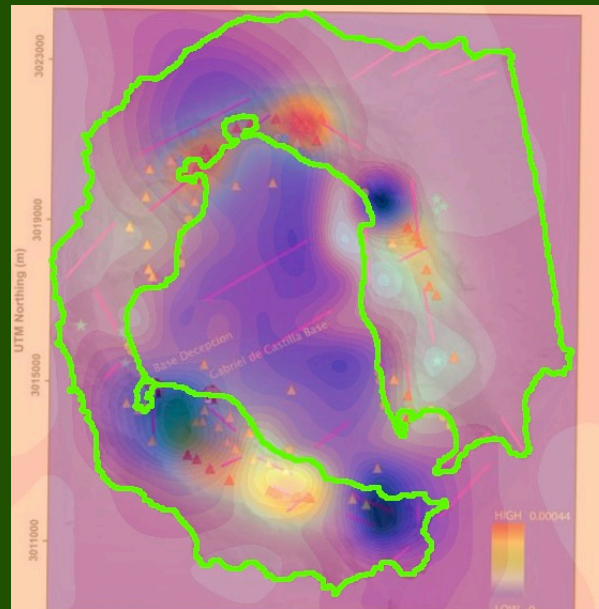
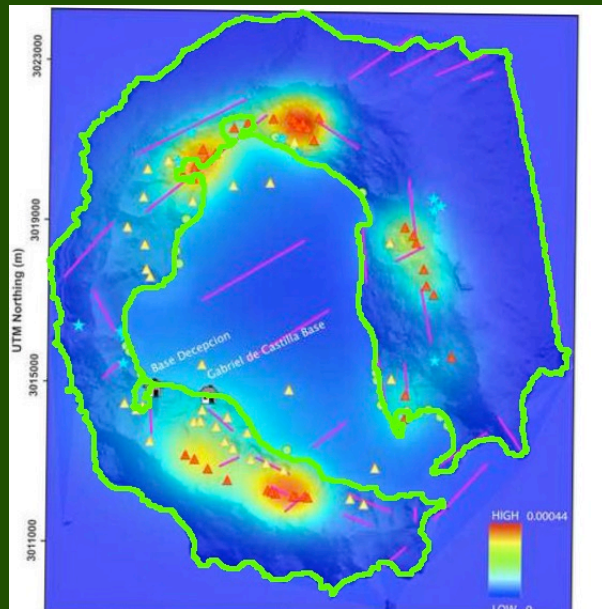
Bartolini et al. 2014 – Fig. 1A  
Simplified regional tectonic map.



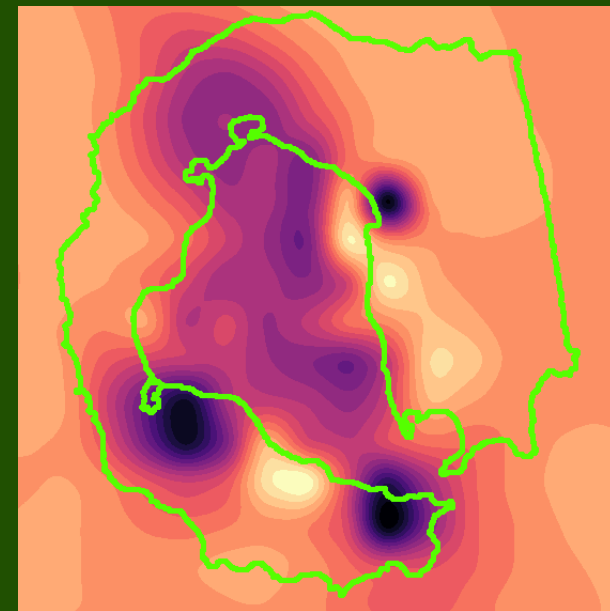
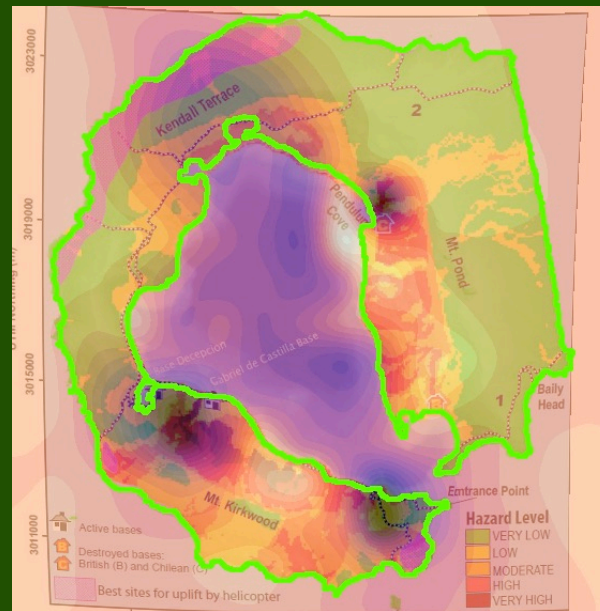
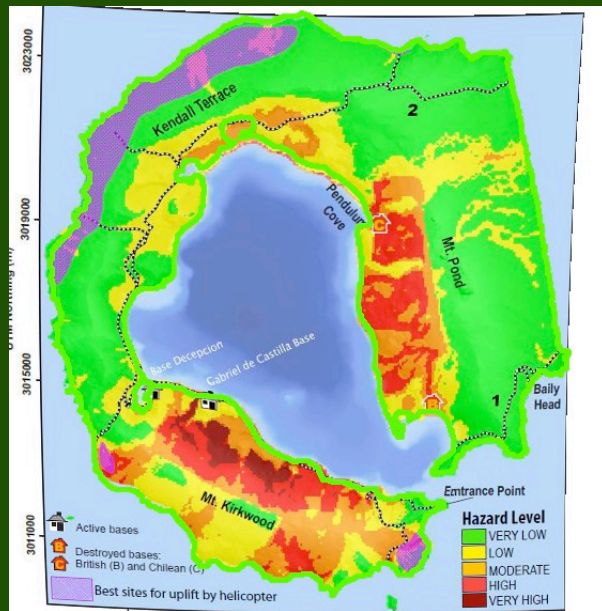


Bartolini et al. 2014 – Fig. 1B

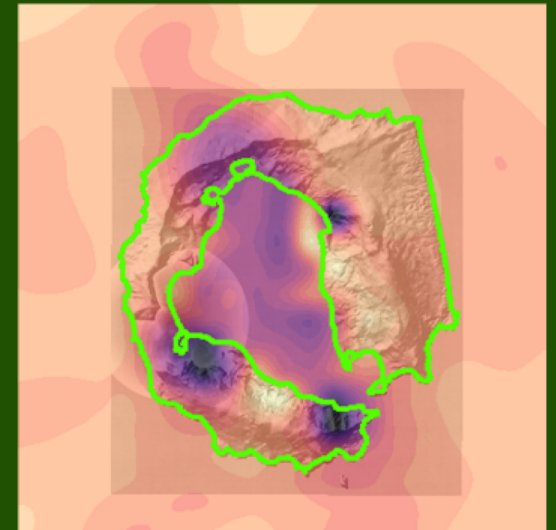
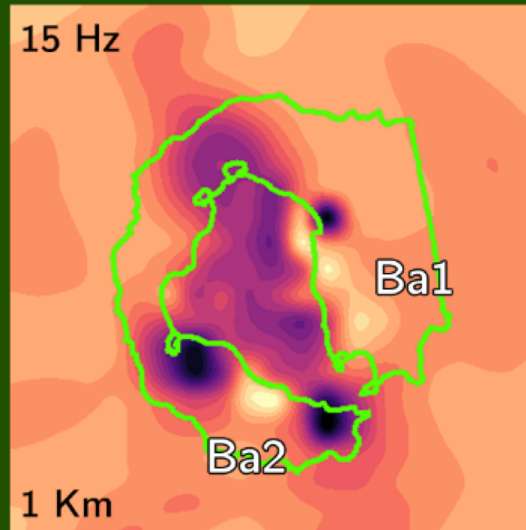
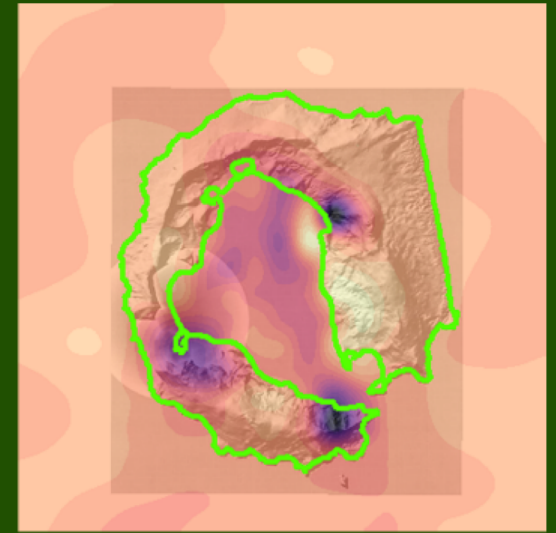
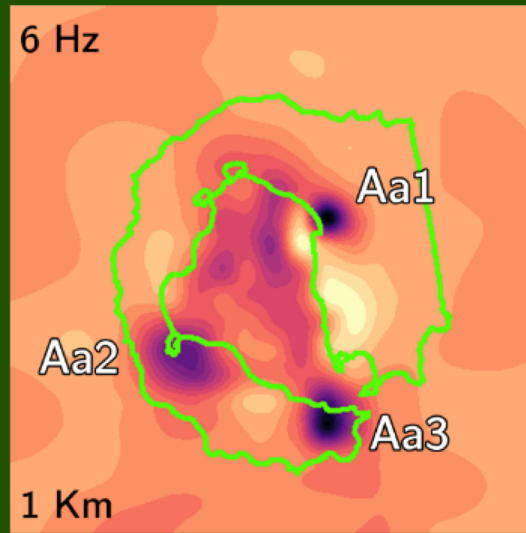
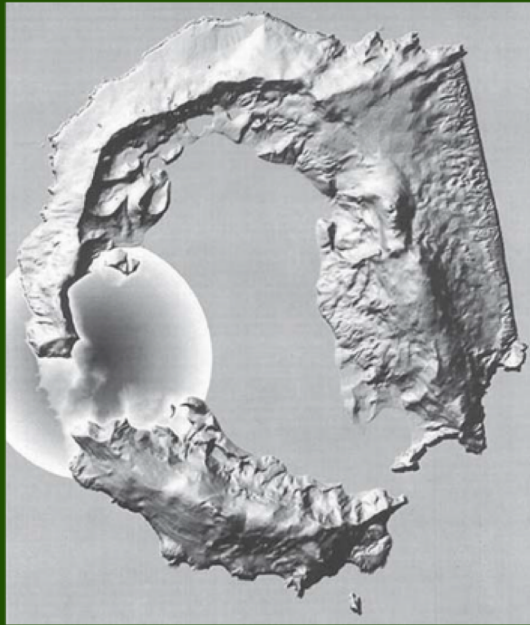




Bartolini et al. 2014 – Fig. 7  
Susceptibility map of future eruptions calculated with QVAST

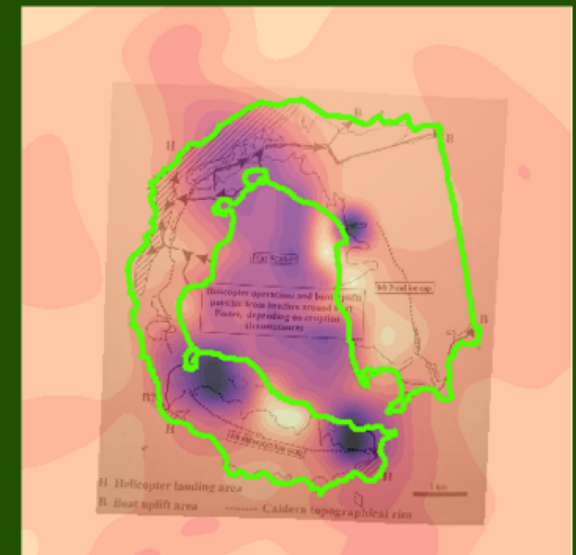
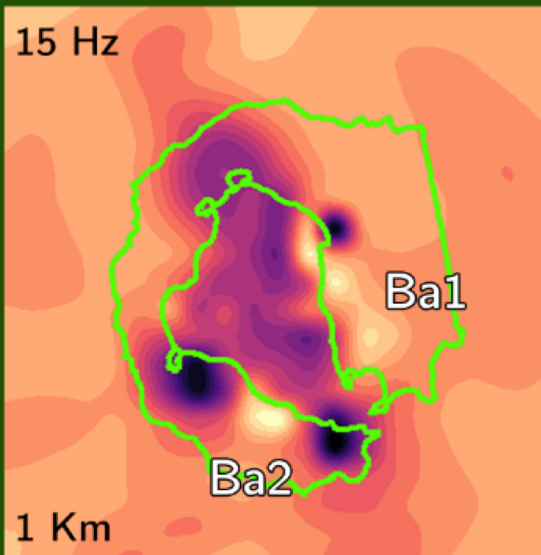
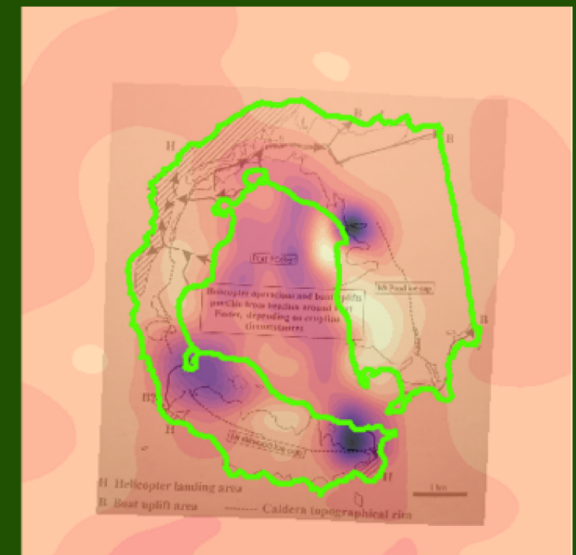
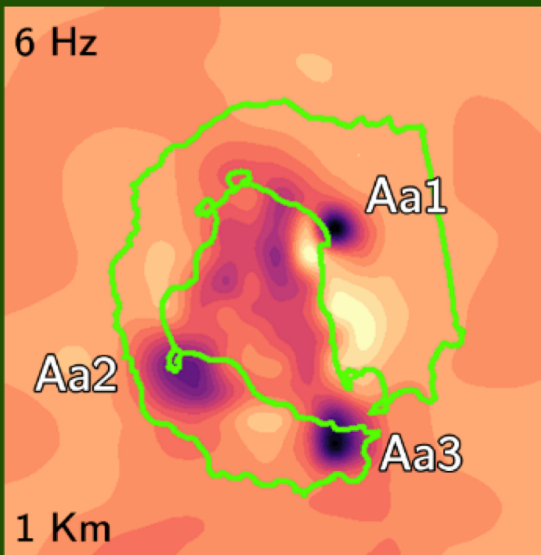
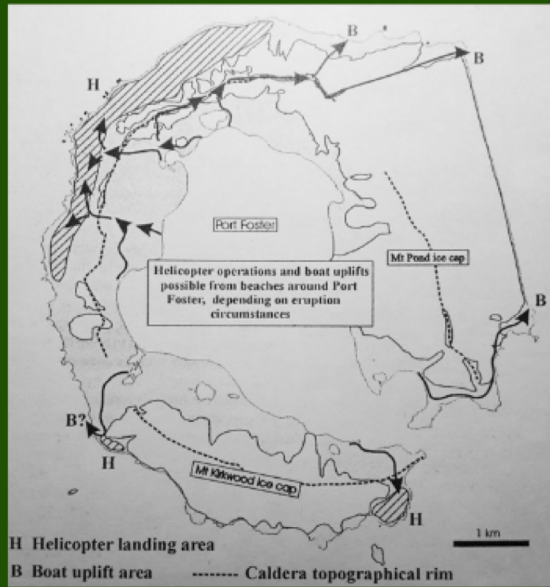


Bartolini et al. 2014 – Fig. 12  
Qualitative hazard map



Berrocso et al. 2006 – Fig. 5.10-6  
Map of natural hazards





Smellie et al. 2002 – Fig. 6.3  
Suggested escape route. The extraction point H (SE) spatially matches the high attenuation area Aa3.

# OUTLOOKS (1)

## at Deception Island Volcano

1. Repeat the analysis using different Coda Windows;
2. 4D analysis;

# OUTLOOKS (2)

## Method application

1. Apply to other volcanoes the aforementioned combination between Qc-Kernel and GIS analysis;
2. Apply the dataset cleaning procedure to other big and high-dimensional data.





**Thanks  
For the  
Attention**